Electrical Power and Energy Systems 133 (2021) 107251

Contents lists available at ScienceDirect

International Journal of Electrical Power and Energy Systems

journal homepage: www.elsevier.com/locate/ijepes

Distributed secondary consensus fault tolerant control method for voltage and frequency restoration and power sharing control in multi-agent microgrid

Bilal Naji Alhasnawi [a], Basil H. Jasim [a], Bishoy E. Sedhom [b,*]

[a] University of Basrah, Faculty of Engineering, Electrical Engineering Department, Basrah 61001, Iraq
[b] Mansoura University, Faculty of Engineering, Electrical Eng. Dept., Mansoura 35516, Egypt

ARTICLE INFO

Keywords:
Fault-tolerant control
Consensus algorithm
Microgrid
Power sharing control
Voltage control
Frequency control

ABSTRACT

This paper proposes a distributed secondary consensus fault-tolerant control (FTC) method for the multi-agent microgrid (MG). The proposed controller is applied to compensate for the errors in the system frequency and voltage profiles in the presence of MG faults. The proposed controller also enables the system to ensure an accurate sharing of the active and reactive power among the connected distributed generations (DGs) in MG. The consensus-based controller depends on the information transferring between MG neighbor agents through a graph communication network. The proposed secondary controller improves the primary controllers' performance, including droop control and inner voltage and current controllers. The proposed controller has been verified using a hypothetical multi-agent MG system in MATLAB/Simulink environment. A comparative analysis between the results obtained from applying the proposed controller and the primary droop control method (DCM). The proposed controller's performance is evaluated using the controller response time, the maximum frequency deviation, and the steady-state restoration time. The results show the proposed secondary FTC method's effectiveness in mitigating the faults' effect in multi-agent MG.

1. Introduction

Nowadays, renewable energy sources (RESs) have been widely used to improve the existing electric power grids' performance. The RESs are an effective solution to mitigate traditional fossil fuels' impacts and increased carbon dioxide emission [1]. Microgrids are a cluster of RESs, energy battery storage units (EBSUs), and loads that operate with integration or isolation from the low voltage distribution networks (LVDNs) [2]. The large-scale use of the MGs in the LVDNs results in a reduction in pollution, minimizing the transmission system losses, improving the system reliability, enhancing the stability, tackling the impacts of harmonics in the system [3]. One of the main challenges related to the MGs is the control of the voltage, frequency, and active and reactive power under its isolated operation and in the presence of the system fault disturbances. The MG faults have devastating effects on its efficiency, performance, steady-state operation, and the data and information exchange in MG. The MG faults are different from the traditional grid as the MG is interfaced with inverters for the connected DGs. The fault current must be limited between 12 and 2 times that of the rated current [4]. The current level of MG faults is changed concerning the MG operating modes; islanded or grid-connected. Also, with the increasing penetration of DGs in MG, the fault current may be bidirectional [4]. The MG faults can be categorized as the actuators' faults, faults in sensors, communication system faults, plant faults, and short circuit faults [5]. This paper focuses on the short-circuit faults that may occur in the MG system. The FTCs are designed to ensure steady-state operation, enhance MGs' fault resilience, and improve MGs' robust and efficient operation.

The severe disturbances and faults affect the DGs connected to the MGs. These disturbances are considered a big challenge for the microgrid controller. After the severe disturbances and faults, the connected DGs are enforced to disconnect from the network and hence affect the stability, reliability, and continuity of service. Recently, with the high integration of the RESs in the system, each DG must be equipped with a FTC mechanism to enhance the MG resiliency in the presence of the low voltage condition for a short time [6]. The FTC provides the MG's interfacing voltage source converter (VSC) the capability to maintain the MG connection and provide the voltage and frequency stability despite the transient short-circuit faults [7].

The main purpose of using the distributed controller is to overcome

* Corresponding author.
E-mail addresses: bilalnaji11@yahoo.com (B.N. Alhasnawi), hanbas632@gmail.com (B.H. Jasim), eng_bishoy90@mans.edu.eg (B.E. Sedhom).

https://doi.org/10.1016/j.ijepes.2021.107251
Received 22 August 2020; Received in revised form 20 March 2021; Accepted 8 May 2021
Available online 4 June 2021

Nomenclature

Abbreviations & Acronyms

FTC	Fault-Tolerant Control
MG	Microgrid
DGs	Distributed Generations
DCM	Droop Control Method
RESs	Renewable Energy Sources
EBSUs	Energy battery storage units
LVDNs	Low voltage distribution networks
LM	Laplacian matrix
TL-G	Three-line to ground fault
SL-G	Single line to ground fault
L-L	Line to line fault
DL-G	Double line to ground
MG-*VF*	Microgrid-Voltage and frequency

Variables & Parameters

ϖ_{ij}	Weighted factors
$\mathcal{K}_i$	Set of agents connected to unit$i$
l_{ii} and l_{jj}	Laplacian matrix
a_{ij}	Number of the incoming communication links
$\mathcal{D}$	Diagonal elements matrix
$\mathcal{A}$	Off-diagonal matrix
k_{pdi} and k_{qdi}	Droop coefficients
ω_i	Angular frequency of i^{th} DG
P_i	Active power (in kW)
Q_i	Reactive power (in $kVAr$)
V_{iref}	Reference voltage
ω_{iref}	Reference frequency
v_{odi}	Direct components of $\mathcal{V}_{oi}$
v_{oqi}	Quadrature components of $\mathcal{V}_{oi}$
i_{odi}	Direct components of i_{oi}
i_{oqi}	Quadrature components of i_{oi}
ϕ_{di}	Direct subsidiary status variables connected to the voltages power PI
ϕ_{qi}	Quadrature subsidiary status variables connected to the voltages power PI
γ_{di}	Direct auxiliary states associated with the new control PI
γ_{qi}	Quadrature auxiliary states associated with the new control PI
v_{bdi}	Direct microgrid bus voltage v_b
v_{bqi}	Quadrature microgrid bus voltage v_b
n	Number of agents
k	Sample time instant
$\Im_{\mathcal{Q}i}(t)$	Reactive power-sharing compensation coefficient
$k_{\mathcal{Q}p}$ and $k_{\mathcal{Q}i}$	Reactive power PI controller gains
$\mathcal{Q}_i^{k+1}(t)$	Value of reactive power at iteration $k+1$
$\mathcal{Q}_i$	Measured reactive power of the DG_i
ξ_i	Reactive power-sharing disturbance at DG_i
$\Im_{\mathcal{V}i}^{k}(t)$	Voltage compensation coefficient for the DG_i
k_{vp} and k_{vi}	Voltage PI controller gains
$\mathcal{V}_i^{k+1}(t)$	Value of reactive power at iteration $k+1$
$\mathcal{V}_{rms}^{*}$	Measured voltage at each DG_i
ζ_i	Voltage disturbance at DG_i
$\Im_{\mathcal{P}i}^{k}(t)$	Active power-sharing compensation coefficient for the DG_i
$k_{\mathcal{P}p}$ and $k_{\mathcal{P}i}$	Active power PI controller gains
$\mathcal{P}_i^{k+1}(t)$	Value of active power at iteration $k+1$
$\mathcal{P}_i$	Measured active power of the DG_i
ϱ_i	Reactive power-sharing disturbance at DG_i
$\Im_{\omega i}^{k}(t)$	Angular frequency compensation coefficient for the DG_i
k_{fp} and k_{fi}	Angular frequency PI controller gains
$\omega_i^{k+1}(t)$	Value of angular frequency at iteration $k+1$
ω^{*}	Measured angular frequency at each DG_i
τ_i	Angular frequency disturbance at DG_i
m_p	Frequency droop parameter
n_Q	Voltage droop parameter
L_f	Filter damping inductance
R_f	Filter damping resistor
Z_{Line}	Line impedance

the problems of centralized control approaches. The centralized controllers suffer from the complex structure of the information transferring network and require a central computing and control unit in the MG [8]. Also, the centralized controller needs two-way communication links with an increased cost. Hence, the controller's reliability is reduced, and failure sensitivity is increased [9]. The distributed control approach is used to eliminate the aforementioned drawbacks related to the central controller. It can use the information and data from the neighbors through a graph communication network. It enhances system reliability, minimizes the sensitivity to the system failure, and mitigates the central control unit's need [10]. The distributed secondary controller provides the system with plug and play capability, enhances the system security, improves the system scalability, enables efficient data and information transfer between the system agents, and fast in operation and decision making [11].

In this paper, a secondary distributed FTC method is proposed based on a consensus algorithm. This secondary control method is proposed to enhance the primary controller's performance, including droop control, voltage, and current controllers. The proposed controller can compensate for the errors in the MG voltage and frequency (MG-VF) signals, and hence the nominal values are achieved under the presence of system faults and disturbances. The proposed controller also enables the proper adjustment of the equally shared active and reactive power among the connected DGs in the MG. In this paper, the proposed secondary control method is applied to tackle the impacts of the short circuit faults that may occur in the transmission lines in MG. In this proposed controller, the MG elements are considered as a multi-agent system with a communication system between these agents. The consensus controller is based on data and information transfer between the agent and its neighbors, depending on the graph communication network. For the sake of comparison, the effectiveness of the proposed controller is measured by comparing the obtained results using the proposed control method with the conventional droop controller. The proposed controller's performance is evaluated based on the controller response time, the maximum frequency deviation, and the steady-state restoration time.

The main contribution of this paper can be summarized as follows;

(1) Proposing a distributed secondary consensus-based control method for the multi-agent MG to improve the primary controller to mitigate the effect of the short circuit faults in the MG transmission system.
(2) Compensating the error in the MG-*VF* waveforms in the presence of the MG's faults and adjust the MG-*VF* to their nominal values.
(3) Ensuring the accurate sharing of the active and reactive power for the connected DGs in MG under the presence of system faults.
(4) Performing a comparative analysis between the proposed controller and the conventional DCM to prove its effectiveness.
(5) Evaluating the proposed controller's performance based on the controller response time, the maximum frequency deviation, and the steady-state restoration time.

This paper is organized as follows; Section 2 represents the

Table 1
Contributions Vs. shortcomings of the most recent researches concerning FTC based consensus algorithm.

Reference	Contributions	Shortcomings
[5]	■ Proposing a secondary consensus FTC based on a sliding mode controller to regulate the MG-VF under the existence of disturbances and actuator faults.	■ The transmission system short circuit faults are not considered.
[23]	■ Introducing a secondary FTC based on a consensus algorithm for MG-VF restoration and active power-sharing among the DGs and EBSUs under the existence of the actuator system faults.	■ The information and data sharing are limited to only local neighbors. ■ The transmission system short circuit faults are not considered.
[24]	■ Proposing a leader-following consensus algorithm-based neural network learning strategy to eliminate the effect of actuator faults in a multi-agent system.	■ The transmission system short circuit faults are not considered. ■ The active and reactive power-sharing are not investigated. ■ The voltage and frequency regulations are not considered
[28]	■ Investigating a secondary consensus controller for MG-VF restoration under the existence of actuator and sensor faults.	■ The transmission system short circuit faults are not considered.
[29]	■ Proposing an adaptive secondary FTC method to improve the voltage restoration under the existence of the sensor faults.	■ The reactive power-sharing is not investigated. ■ The transmission system short circuit faults are not considered.
[30]	■ Introducing an event-triggered consensus control method to mitigate the communication faults in the DC microgrids while regulation the system voltage to its nominal value	■ The frequency regulation is not considered. ■ The active and reactive power sharing is not investigated. ■ The inner control loops are not investigated. ■ The transmission system short circuit faults are not considered.
[31]	■ Proposing a leader-following consensus controller for a multi-agent system to eliminate the effect of the actuator faults while using the neural network as a learning algorithm to estimate the actuator faults unknown limits.	■ The voltage and frequency regulation are not considered. ■ The active and reactive power sharing is not investigated. ■ The primary control loop is not investigated. ■ The transmission system short circuit faults are not considered.
[32]	■ Presenting a consensus-based control method to mitigate the transmission communication system's delay while enhancing the system voltage in AC microgrids.	■ The frequency regulation is not considered. ■ The transmission system short circuit faults are not considered.
[33]	■ Proposing a sliding mode controller based on the leader consensus algorithm for a multi-agent system to mitigate the effect of the actuator faults and disturbances while enhancing the sliding mode controller's performance by adequately adjusting the control gain automatically.	■ The voltage and frequency regulation are not considered. ■ The active and reactive power sharing is not investigated. ■ The current and voltage control loops are not investigated. ■ The transmission system short circuit faults are not considered.
[34]	■ Introducing a consensus FTC method for the multi-agent system to tackle the actuator faults' impact while reducing the consensus error to zero for the leader–follower system.	■ The information and data sharing are limited to only local neighbors. ■ The voltage and frequency regulation are not considered. ■ The active and reactive power sharing is not investigated. ■ The current and voltage control loops are not investigated. ■ The transmission system short circuit faults are not considered.
[35]	■ Proposing a FTC method based on a consensus algorithm for the nonidentical high-order multi-agent system to eliminate the effect of the actuator faults and system network disconnections.	■ The voltage and frequency regulation are not considered. ■ The active and reactive power sharing is not investigated. ■ The inner control loops are not investigated. ■ The transmission system short circuit faults are not considered.
[36]	■ Proposing a consensus-based FTC method is proposed for the multi-agent system to compensate for the effect of actuation failure, uncertainties, and system disturbances by considering the agents' information exchange.	■ The information and data sharing are limited to only local neighbors. ■ The voltage and frequency regulation are not considered. ■ The active and reactive power sharing is not investigated. ■ The current and voltage control loops are not investigated. ■ The transmission system short circuit faults are not considered.
[37]	■ Presenting a consensus control method for false data injection attacks in the DC MGs while enhancing the DC voltage and proposing a discrimination method between the cyberattack and system faults.	■ The active and reactive power sharing is not investigated. ■ The transmission system short circuit faults are not considered.
Our Work	■ Proposing a distributed secondary consensus-based control method for the multi-agent MG to improve the primary controller to mitigate the effect of the short circuit faults in the MG transmission system. ■ Compensating the error in the MG-VF waveforms in the presence of the system faults in the MG and adjusting the MG-VF to their nominal values. ■ Ensuring the accurate sharing of the active and reactive power for the connected DGs in MG under the presence of the system faults. ■ Evaluating the proposed controller's performance based on the controller response time, the maximum frequency deviation, and the steady-state restoration time.	■ Investigating a secure cloud-based platform for multi-agent's hybrid AC/DC MG-FTC is considered our future work.

mathematical model of information transferring graph network. Section 3 introduces the primary control method, including droop controller, voltage, and current control loops. Section 4 represents the proposed distributed secondary consensus FTC method for the multi-agent MGs. The system modeling and simulation results are introduced in Section 6, while Section 7 describes the results' discussion and analysis. Finally, Section 8 concludes the paper.

2. Related work

Different control methods are applied to mitigate the effects of system faults in the MGs. These control methods as; multi-agent system control (MAS) [12–13], sliding mode control (SMC) [6,14–15], reinforcement learning algorithm [16–17], model predictive control (MPC) [18–20], H-infinity (H∞) control [21–22], and consensus control [23–24]. In literature, authors in [12] proposed a secondary FTC method based on MAS capable of operating either in a semi-centralized or distributed manner to optimal coordinate the microgrid units and restore voltage and frequency and obtain the optimal droop coefficients. In [13], authors introduced a semi-centralized and distributed FTC method based on a hybrid MAS for voltage and frequency restoration and microgrid unit's coordination in the presence of system fault and system reconfiguration. In [6], the authors proposed a neural SMC to regulate the active and reactive power generated in a microgrid. This controller applied the recurrent neural network identification, which has been trained online with an extended Kalman filter algorithm. Authors in [14] introduced a new paradigm FTC system for a double-fed induction generator (DFIG) based wind system connected to a microgrid to enable the strict satisfaction of recent grid code requirements and achieve ride through during any voltage sag conditions, including deep sags. Also, in [15], the authors proposed a FTC method based on SMC for heterogeneous MASs with matched disturbances, unmatched nonlinear interactions, and actuator faults to ensure the stability of the MASs. In [16], the authors proposed an adaptive FTC for discrete-time MAS class

by a reinforcement learning algorithm. In this controller, action neural networks (NNs) are used to approximate the unknown control input signal, while critic NNs are used to estimate the design procedure costs. In [17], authors introduced a new method to damp the voltage and frequency oscillations in the microgrid using wind turbine generator penetration (WTG) based on a reinforcement learning algorithm with FTC capability. Authors in [18] proposed a FTC of microgrid based on MPC synthesized upon a linear parameter varying (LPV) prediction model to maximize the sharing of RESs and enlarge the maximum efficiency and profit in the presence of system faults. In [19], a control strategy with the fault ride-through capability is introduced to regulate the current reference of the DFIG and adjust the active power-sharing. In [20], authors proposed a FTC on an industrial energy microgrid based on MPC and moving horizon estimate (MHE) paradigm for fault estimation to achieve maximum profit while ensuring that the demand is met under system fault impact and different operational constraints. Authors in [21] proposed a control strategy for the autonomous operation adjustment of MG based on H∞ control with FTC capability to improves system power quality and adjust the MG voltage and frequency at their specified values in the presence of short circuit faults. In [22] introduced two novel FTC algorithms to restore voltage and frequency in autonomous inverter-interfaced AC microgrid based on H∞ control in the presence of various potential failures in sensors and actuators. In [23], the authors introduced a secondary FTC based on a consensus algorithm for MG-VF restoration and active power-sharing among the DGs and EBSUs under the existence of the actuator system faults. Authors in [24] proposed a leader-following consensus algorithm-based neural network learning strategy to eliminate the effect of actuator faults in a multi-agent system. Also, a comparison between the pros and cons of these control methods is represented in Appendix A.

One of the main fault-tolerant controllers is the consensus control algorithm. The consensus controller is an iterative interaction method that can exchange the data and data among the agents and all their neighbors in the MG [25]. This controller enables the MG agents to coordinate and hence ensures transferring the information between these agents locally. It is a promising control method in solving the large coordination problems in MGs [26]. Also, the consensus controller is a distributed controller. It has valuable advantages, including ease in the implementation, flexibility in operation, efficient computation, adaptive to variation in system topology, and the MG plug-and-play capability [27]. Table 1 involves the contributions and shortcomings of the most recent research applied to eliminate the impact of system faults in the MGs based on consensus control algorithm.

Researchers in [5,23,24,28–37] have recently proposed several forms of distributed consensus control methods for achieving a stable operation in MG. However, there are limitations to the existing control approaches as follows;

(1) Neglecting the changes in system load demand, line impedances, the MG configuration, and the inputs to the DGs connected to the MG. These parameters are considered as uncertainties and disturbances that may be accomplished with the MG system.
(2) Do not consider the inner control loops such as the current and voltage controllers. However, the inner voltage and current controllers are necessary to enhance the system voltage and current concerning system disturbances.
(3) Performing the system control design and its performance without a concentration in the system parameters improvement under the presence of system disturbances.
(4) Concentrating on the actuator, noise, and communication failure faults without considering the short circuit faults that may occur in the transmission lines in MG.
(5) Enhancing the MG-*VF* in the presence of system faults and ensuring active and reactive power-sharing is not considered.
(6) Neglecting the performance measurement of the proposed controller-based on the time response, system performance indices, and maximum frequency deviation.

3. Information transferring network for the proposed distributed consensus control

The MG system is considered a multi-agent system with information capability transfer between the local device and the neighbors to obtain an efficient distributed consensus controller for MG fault mitigation. MG elements such as; DGs, loads, and inverters are connected to the distributed consensus controller, and the distributed consensus controller can communicate with neighbors to obtain an optimal decision for the local element. The flow diagram of the information between these agents can be represented as an undirected graph, including the nodes and the edges. Each agent in the distributed consensus control can be described as a node, and the information communication links between agents i and j can be represented as an edge (i,j) with w_{ij} weighted factor. Hence the graph of the information flow diagram can be represented as $\mathcal{G} = \{\mathcal{N}, \mathcal{E}, \mathcal{A}\}$ where $\mathcal{N} = \{1, \cdots, \mathcal{K}\}$ is the number of agents in the MG system, $\mathcal{E}$ is the communication links between two adjacent agents, $\mathcal{E}(i,j)$, and $\mathcal{A} \in \mathcal{R}^{\mathcal{K}\times\mathcal{K}}$ is the weighted matrix. The undirect graph means that the information transferring capability is from the controllers at agents i and j and vice versa hence, the set of neighbors of the controller $i \in \mathcal{N}$ can be denoted as $\mathcal{K}_i = \{j : j \in \mathcal{N}, (i,j) \in \mathcal{E}\}$. The w_{ij} weighted factors can be represented as follows [3];

$$w_{ij} = \begin{cases} 1/(max[l_{ii}, l_{jj}] + 1) & j \in \mathcal{K}_i \\ 1 - \sum_{j \in \mathcal{K}_i} 1/(max[l_{ii}, l_{jj}] + 1) & j = i \\ 0 & otherwise \end{cases} \quad (1)$$

where i and j are units' number, $\mathcal{K}_i$ is the set of agents connected to unit$i$, and l_{ii} and l_{jj} are the Laplacian matrix (LM) component. The elements of the LM can be represented as follows [5];

$$\begin{cases} l_{ii} = \sum_{i \neq j} a_{ij} & on - diagonal\ \ elements \\ l_{ij} = -a_{ij} & off - diagonal\ \ elements \end{cases} \quad (2)$$

where, $a_{ij} = 1$ if a communication link between nodes i and j is existed, meanwhile $a_{ij} = 0$. l_{ii} is the number of the incoming communication links at node i. The graph LM is represented as $\mathcal{L} = \mathcal{D} - \mathcal{A}$ in which $\mathcal{D} = Diag\{l_{ii}\}$ and $\mathcal{A} = [a_{ij}]$ where $\mathcal{D}$ is a diagonal elements matrix and $\mathcal{A}$ is an off-diagonal matrix.

4. Primary control of inverter-based DG

Each DG unit's primary control is based on the power, voltage, and current control loops. The main objective of using power control is to ensure proper power-sharing between the DGs meanwhile, providing the reference MG-*VF* to the voltage and current controllers. The power controller depends on the droop control designed based on the strong coupling between the frequency and active power and the voltage and reactive power. The voltage controller is applied for obtaining the reference current required to the current controller; however, the current controller is used for ensuring the reference voltage for the voltage source converter (VSC). The droop controller can be represented as follows [22];

$$\begin{cases} w_i = w_i^{ref} - k_{pdi} P_i \\ v_{odi}^{*} = V_i^{ref} - k_{qdi} Q_i \\ v_{oqi}^{*} = 0 \end{cases} \quad (3)$$

where $k_{pdi}$and k_{qdi} are the droop coefficients; ω_i is the angular frequency of i^{th} DG unit; P_i and Q_i denote the active power (in kW) and reactive

power (in *kVAr*) measured at the terminals of i^{th} DG respectively; V_{iref} and ω_{iref} act as the reference MG-*VF* signals, respectively.

The selection of the droop controller coefficient depends on the active and reactive power ratings of each DG. The power calculation equations and the voltage and current controllers' equations are represented in [38]. The differential–algebraic equations of the voltage controller are given as follows [38];

$$\begin{cases} \dot{\phi}_{d\prime} = \mathscr{V}^{*}_{od\prime} - \mathscr{V}_{od\prime} \\ \dot{\phi}_{q\prime} = \mathscr{V}^{*}_{oq\prime} - \mathscr{V}_{oq\prime} \\ \dot{\prime}^{*}_{ld\prime} = F_{\prime} i_{od\prime} - \omega_b C_{fi} \mathscr{V}_{oq\prime} + K_{pv\prime}(\mathscr{V}^{*}_{od\prime} - \mathscr{V}_{od\prime}) + K_{Iv\prime}\phi_{di} \\ \dot{\prime}^{*}_{lq\prime} = F_{i} i_{oq\prime} + \omega_b C_{fi} \mathscr{V}_{od\prime} + K_{pv\prime}(\mathscr{V}^{*}_{oq\prime} - \mathscr{V}_{oq\prime}) + K_{Iv\prime}\phi_{qi} \end{cases} \tag{4}$$

where $v_{od\prime}$, $v_{oq\prime}$, $\prime_{od\prime}$ and $\prime_{oq\prime}$ are the direct and quadrature components of $\mathscr{V}_{o\prime}$, $\prime_{o\prime}$. Also, ϕ_{di} and ϕ_{qi} are subsidiary status variables connected to voltages power PI controllers and where the nominal angular frequency is denoted by ω_b. The current controller equations are also represented as follows [38];

$$\begin{cases} \dot{\gamma}_{di} = i^{*}_{ldi} - i_{ldi} \\ \dot{\gamma}_{qi} = i^{*}_{qi} - i_{qi} \\ v^{*}_{idi} = -\omega_b L_{fi} i_{lqi} + K_{Pri}(i^{*}_{ldi} - i_{ldi}) + K_{Ici}\gamma_{di} \\ v^{*}_{iqi} = \omega_b L_{fi} i_{ldi} + K_{Pci}(i^{*}_{lqi} - i_{lqi}) + K_{Ici}\gamma_{qi} \end{cases} \tag{5}$$

where $\gamma_{di}$and γ_{qi} are the auxiliary states associated with the new control PI controllers. Finally, the output LCL filter and coupling circuit equations are represented as follows [38];

$$\begin{cases} \dot{i}_{ldi} = -\dfrac{R_f}{L_{fi}} i_{di} + \omega_i i_{qqi} + \dfrac{1}{L_{fi}} v_{idi} - \dfrac{1}{L_{fi}} v_{odi} \\ \dot{i}_{lqi} = -\dfrac{R_f}{L_{fi}} i_{qi} - \omega_i i_{ldi} + \dfrac{1}{L_{fi}} v_{iqi} - \dfrac{1}{L_{fi}} v_{oqi} \\ \dot{v}_{odi} = \omega_i v_{oqi} + \dfrac{1}{C_{fi}} i_{ldi} - \dfrac{1}{c_{fi}} i_{odi} \\ \dot{v}_{oqi} = -\omega_i v_{odi} + \dfrac{1}{C_{fi}} i_{lqi} - \dfrac{1}{C_{fi}} i_{oqi} \\ \dot{i}_{odi} = -\dfrac{R_{cl}}{L_{ci}} i_{odi} + \omega_i i_{oqi} + \dfrac{1}{L_{cl}} v_{odi} - \dfrac{1}{L_{cl}} v_{bdi} \\ \dot{i}_{oqi} = -\dfrac{R_{ci}}{L_{ci}} i_{oqi} - \omega_i i_{odi} + \dfrac{1}{L_{ci}} v_{oqi} - \dfrac{1}{L_{ci}} v_{bqi} \end{cases} \tag{6}$$

where $v_{bdi}$and v_{bqi} are direct microgrid bus voltage v_b and quadrature elements.

The primary control can't regulate the system MG-*VF* and ensure accurate power-sharing in load changing and system disturbances. The secondary control method is required to enhance the MG's performance and ensure steady-state operation concerning the existence of system disturbances.

5. Proposed distributed secondary consensus-based Fault-Tolerant control (FTC) method

In this paper, the FTC method is proposed to overcome the impacts of faults in the MG based on a distributed consensus control method. The proposed controller can restore the system frequency, voltage, active and reactive power -sharing between DGs in MG. In this method, the MG system is considered a multi-agent system with a communication system between these agents for local neighborhood tracking of voltage, frequency, and active and reactive power errors. The consensus algorithm communicates with all neighbors to adjust the MG-VF and ensure accurate active and reactive power-sharing between the connected DGs in MG.

The consensus control method is proposed to overcome the influences of the system fault in MG. This controller can exchange local information between the neighboring agents. Each DG can receive information from the neighboring agents such as voltage, frequency, active power, and reactive power. The proposed controller aims to enhance the MG-*VF* in the presence of system fault and ensure accurate active and reactive power-sharing among the connected DGs. Each DG update their information concerning the information states received from the neighboring agents. The consensus control objective is to enable the information states of each connected DG to converge at a prescribed value with an iterative form. The discrete-time representation of the iterative based consensus control algorithm can be written as follows;

$$\mathscr{X}^{\mathscr{k}+1}_{\prime}(\prime) = \mathscr{X}^{\mathscr{k}}_{\prime}(\prime) + \sum\nolimits_{\jmath=1}^{n} \omega_{\prime\jmath}(\mathscr{X}^{\mathscr{k}}_{\jmath}(\prime) - \mathscr{X}^{\mathscr{k}}_{\prime}(\prime)) \tag{7}$$

where n is the number of agents in MG, ω_{ij} is the communication transferring capability weight between nodes $\prime$ and$\jmath$, and $\mathscr{k}$ is the sample time instant.

The proposed controller is a distributed control that is equipped with each DG unit in the MG. The proposed control method consists of a primary controller based on droop and voltage and current controllers and a secondary controller based on the consensus control method for adjusting MG-*VF* and ensuring active and reactive power-sharing. The proposed controller's main objective is to overcome the fault effects in MG while regulating the MG-*VF* and obtaining an accurate power-sharing. The following subsections discuss the mathematical formulation of the proposed control method.

The proposed secondary consensus-based controller consists of two regulation control method. The first regulation control is to adjust the system voltage to its nominal values and ensure the accurate reactive power-sharing under the system faults. The second regulation control is to restore the system frequency to its prescribed value and enhance active power-sharing among the connected DGs in MG. The following subsections illustrate the proposed secondary consensus-based fault-tolerant controller.

(1) *Secondary fault-tolerant controller for voltage regulation and reactive power-sharing based on the distributed consensus control method*

This secondary fault-tolerant controller is based on adjusting the system voltage and ensuring an accurate reactive power-sharing among the connected DGs. The reactive power doesn't share equally between the DGs using the primary droop controller because of the line impedance that affects the MG buses' voltages. In this controller, the reactive power-sharing is accurately distributed between the connected DGs in the MG while regulating the MG voltages in the presence of the system faults. The consensus controller is based on the communication protocol that has been built using the graph theory in which the information of the reactive power from the neighbors is provided for each DG in the MG. The consensus-based secondary controller for the reactive power-sharing in the presence of system faults can be written as follows;

$$\Im^{\mathscr{k}}_{Qi}(\prime) = \left(\mathscr{C}^{\mathscr{k}+1}_{\prime}(\prime) - \mathscr{C}_{i}\right)\left(\mathscr{k}_{\mathscr{p}\prime} + \frac{\mathscr{k}_{\mathscr{y}\prime}}{s}\right) \tag{8}$$

$$\mathscr{C}^{\mathscr{k}+1}_{\prime}(\prime) = \mathscr{C}^{\mathscr{k}}_{\prime}(\prime) + \sum_{\jmath=1}^{n} w_{\prime\jmath}\left(\mathscr{C}^{\mathscr{k}}_{\jmath}(\prime) - \mathscr{C}^{\mathscr{k}}_{\prime}(\prime)\right) + \xi_i \tag{9}$$

where $\Im_{\mathscr{C}i}(\prime)$ is the reactive power-sharing compensation coefficient for the DG_i, $\mathscr{k}_{\mathscr{p}\prime}$ and $\mathscr{k}_{\mathscr{y}\prime}$ are the reactive power PI controller gains; $\mathscr{k}$ is the consensus algorithm iteration number; $\mathscr{C}^{\mathscr{k}+1}_{\prime}(\prime)$ is the value of reactive power at iteration $\mathscr{k}+1$, $\mathscr{C}_i$ represents the measured reactive power of the DG_i, and ξ_i is the reactive power-sharing disturbance at DG_i. The

Table 2
The consensus FTC for voltage restoration and reactive power sharing control algorithm.

1. System parameters initialization

2. Weighting factor matrix evaluation $w_{i,j}$ using:

$$w_{i,j} = \begin{cases} 1/(max[l_{ii}, l_{jj}] + 1) & j \in \mathcal{K}_i \\ 1 - \sum_{j \in \mathcal{K}_i} 1/(max[l_{ii}, l_{jj}] + 1) & j = i \\ 0 & otherwise \end{cases}$$

3. Update voltage using:

$$\Im_{Vi}^{k}(t) = \left(\mathcal{V}_{rms}^{*} - \mathcal{V}_{i}^{k+1}(t) + k_{q,di}\,\Im_{Qi}^{k}(t)\right)\left(k_{vp} + \frac{k_{vi}}{s}\right)$$

4. **While** $error_v <$ acceptable value ***do***

$$\begin{array}{l} for\ all\ i < N\ do \\ \mathcal{V}_i^{k+1}(t) = \mathcal{V}_i^{k}(t) + \sum_{j=1}^{n} w_{ij}\left(\mathcal{V}_j^{k}(t) - \mathcal{V}_i^{k}(t)\right) + \zeta_i \\ error_{\mathcal{V}_i} = \left|\mathcal{V}_i^{k+1}(t) - \mathcal{V}_i^{k}(t)\right| \\ \textbf{end} \\ error_{\mathcal{V}} = \max\{error_{\mathcal{V}_i}\} \\ \textbf{end while} \end{array}$$

5. Update reactive power:

$$\Im_{Qi}^{k}(t) = \left(\mathcal{Q}_i^{k+1}(t) - \mathcal{Q}_i\right)\left(k_{q,p} + \frac{k_{q,i}}{s}\right)$$

6. **While** $error_Q <$ acceptable value ***do***

$$\begin{array}{l} for\ all\ i < N\ do \\ \mathcal{Q}_i^{k+1}(t) = \mathcal{Q}_i^{k}(t) + \sum_{j=1}^{n} w_{ij}\left(\mathcal{Q}_j^{k}(t) - \mathcal{Q}_i^{k}(t)\right) + \xi_i \\ error_{Qi} = \left|\mathcal{Q}_i^{k+1}(t) - \mathcal{Q}_i^{k}(t)\right| \\ \textbf{end} \\ error_{Q} = \max\{error_{Q_i}\} \\ \textbf{end while} \end{array}$$

main objective of using the PI controller is to enhance the performance of the secondary consensus controller.

Moreover, the secondary fault tolerant voltage controller is proposed based on the consensus control method. This controller regulates the voltage signal to its nominal values by providing the reference voltage to the primary controller V_{iref}. This controller can regulate the system voltage under the existence of the system fault disturbances. The consensus controller provides the information to the entire DG controller from the neighbors through the communication graph $\mathcal{G}$. The proposed consensus-based fault tolerant voltage regulator compensates the output voltage from the impacts of the droop gains and the virtual impedances. The voltage regulator equation can be written as follows;

$$\Im_{\mathcal{V}i}^{k}(t) = \left(\mathcal{V}_{rms}^{*} - \mathcal{V}_{i}^{k+1}(t) + k_{qd,i}\Im_{Qi}^{k}(t)\right)\left(k_{vp} + \frac{k_{vi}}{s}\right) \tag{10}$$

$$\mathcal{V}_{i}^{k+1}(t) = \mathcal{V}_{i}^{k}(t) + \sum_{j=1}^{n} w_{ij}\left(\mathcal{V}_{j}^{k}(t) - \mathcal{V}_{i}^{k}(t)\right) + \zeta_i \tag{11}$$

where $\Im_{\mathcal{V}i}^{k}(t)$ is the voltage compensation coefficient for the DG_i, k_{vp} and k_{vi} are the voltage PI controller gains, $\mathcal{V}_{i}^{k+1}(t)$ is the value of reactive power at iteration $k+1$, $\mathcal{V}_{rms}^{*}$ represents the measured voltage at each DG_i, and ζ_i is the voltage disturbance at DG_i.

The secondary consensus controller mitigates the reactive power-sharing error after evaluating the reactive power-sharing compensation coefficient, according to (8). The consensus controller also adjusts the voltage to its nominal values after estimating the voltage compensation coefficient, according to (10). Hence, the proposed secondary controller regulates the system voltage and ensures an accurate reactive power-sharing in the presence of disturbances in the system voltage, ζ_i, and reactive power, ξ_i. The secondary controller output signal is sent to the primary droop controller as follows;

$$\mathcal{V}_{i}^{ref} = \mathcal{V}_{rms}^{*} + \Im_{\mathcal{V}i}^{k}(t) + k_{qd,i}\Im_{Qi}^{k}(t) \tag{12}$$

(2) ***Secondary fault-tolerant controller for frequency restoration and active power-sharing based on the distributed consensus control method***

Table 3
The consensus FTC for frequency restoration and active power sharing control algorithm.

1. System parameters initialization
2. Weighting factor matrix evaluation $w_{i,j}$ using:

$$w_{i,j} = \begin{cases} 1/(max[l_{ii}, l_{jj}] + 1) & j \in \mathcal{K}_i \\ 1 - \sum_{j \in \mathcal{K}_i} 1/(max[l_{ii}, l_{jj}] + 1) & j = i \\ 0 & otherwise \end{cases}$$

3. Update active power:

$$\Im_{\mathcal{P}i}^{k}(t) = (\mathcal{P}_i^{k+1}(t) - \mathcal{P}_i)\,(k_{pp} + \frac{k_{pi}}{s})$$

4. **While** $error_P <$ acceptable value ***do***

$$for\ all\ i < N\ do$$
$$\mathcal{P}_i^{k+1}(t) = \mathcal{P}_i^{k}(t) + \sum_{j=1}^{n} w_{ij}\,(\mathcal{P}_j^{k}(t) - \mathcal{P}_i^{k}(t)) + \varrho_i$$
$$error_{\mathcal{P}_i} = |\mathcal{P}_i^{k+1}(t) - \mathcal{P}_i^{k}(t)|$$
end
$$error_{\mathcal{P}} = \max\{error_{\mathcal{P}_i}\}$$
end while

5. Update frequency:

$$\Im_{wi}^{k}(t) = (w^* - w_i^{k+1}(t) + k_{pdi}\,\Im_{\mathcal{P}i}^{k}(t))\,(k_{fp} + \frac{k_{fi}}{s})$$

6. **While** $error_w <$ acceptable value ***do***

$$for\ all\ i < N\ do$$
$$w_i^{k+1}(t) = w_i^{k}(t) + \sum_{j=1}^{n} w_{ij}\,(w_j^{k}(t) - w_i^{k}(t)) + \tau_i$$
$$error_{w_i} = |w_i^{k+1}(t) - w_i^{k}(t)|$$
end
$$error_{w_i} = \max\{error_{w_i}\}$$
end while

The proposed secondary consensus control method is applied to enhance the performance of the primary controller. In this controller, the active power-sharing is actually allocated to the connected DGs in the MG; also, the system frequency is restored to its nominal values in the presence of the system disturbances. The information and data are collected from the neighbors for each DG in the MG for an accurate control decision signal. This secondary consensus controller's main objective is to provide the reference angular frequency to the primary DCM for optimally adjusting the system frequency and active power-sharing. The communication protocol is performed using the graph network $\mathcal{G}$ to ensure the data transfer among the connected DGs in MG. The consensus-based distributed fault-tolerant active power controller can be written as follows;

$$\Im_{\mathcal{P}i}^{k}(\ell) = \left(\mathcal{P}_i^{k+1}(\ell) - \mathcal{P}_i\right)\left(k_{pp} + \frac{k_{pi}}{s}\right) \tag{13}$$

$$\mathcal{P}_i^{k+1}(\ell) = \mathcal{P}_i^{k}(\ell) + \sum_{j=1}^{n} w_{ij}\left(\mathcal{P}_j^{k}(\ell) - \mathcal{P}_i^{k}(\ell)\right) + \varrho_i \tag{14}$$

where $\Im_{\mathcal{P}i}^{k}(\ell)$ is the active power sharing compensation coefficient for the DG_i, k_{pp} and k_{pi} are the active power PI controller gains; $\mathcal{P}_i^{k+1}(\ell)$ is the value of active power at iteration $k+1$, $\mathcal{P}_i$ represents the measured active power of the DG_i, and ϱ_i is the reactive power-sharing disturbance at DG_i.

The secondary control layer is proposed to regulate the system frequency based on a distributed consensus controller. The main purpose of the secondary fault-tolerant frequency controller is to provide the conventional droop controller with the reference frequency signal w_i^{ref} to regulate the system frequency deviation from its nominal value under system fault disturbance. In the frequency regulator control, each DG communicates with the neighbors with the data and information through the communication graph $\mathcal{G}$. The secondary distributed consensus frequency control equation can represent as follows;

$$\Im_{wi}^{k}(\ell) = \left(w^* - w_i^{k+1}(\ell) + k_{pdi}\,\Im_{\mathcal{P}i}^{k}(\ell)\right)\left(k_{fp} + \frac{k_{fi}}{s}\right) \tag{15}$$

$$w_i^{k+1}(\ell) = w_i^{k}(\ell) + \sum_{j=1}^{n} w_{ij}\left(w_j^{k}(\ell) - w_i^{k}(\ell)\right) + \tau_i \tag{16}$$

where $\Im_{wi}^{k}(\ell)$ is the angular frequency compensation coefficient for the DG_i, k_{fp} and k_{fi} are the angular frequency PI controller gains, $w_i^{k+1}(\ell)$ is the value of angular frequency at iteration $k+1$, w^* represents the measured angular frequency at each DG_i, and τ_i is the angular frequency disturbance at DG_i.

The active power-sharing is adjusted according to the active power

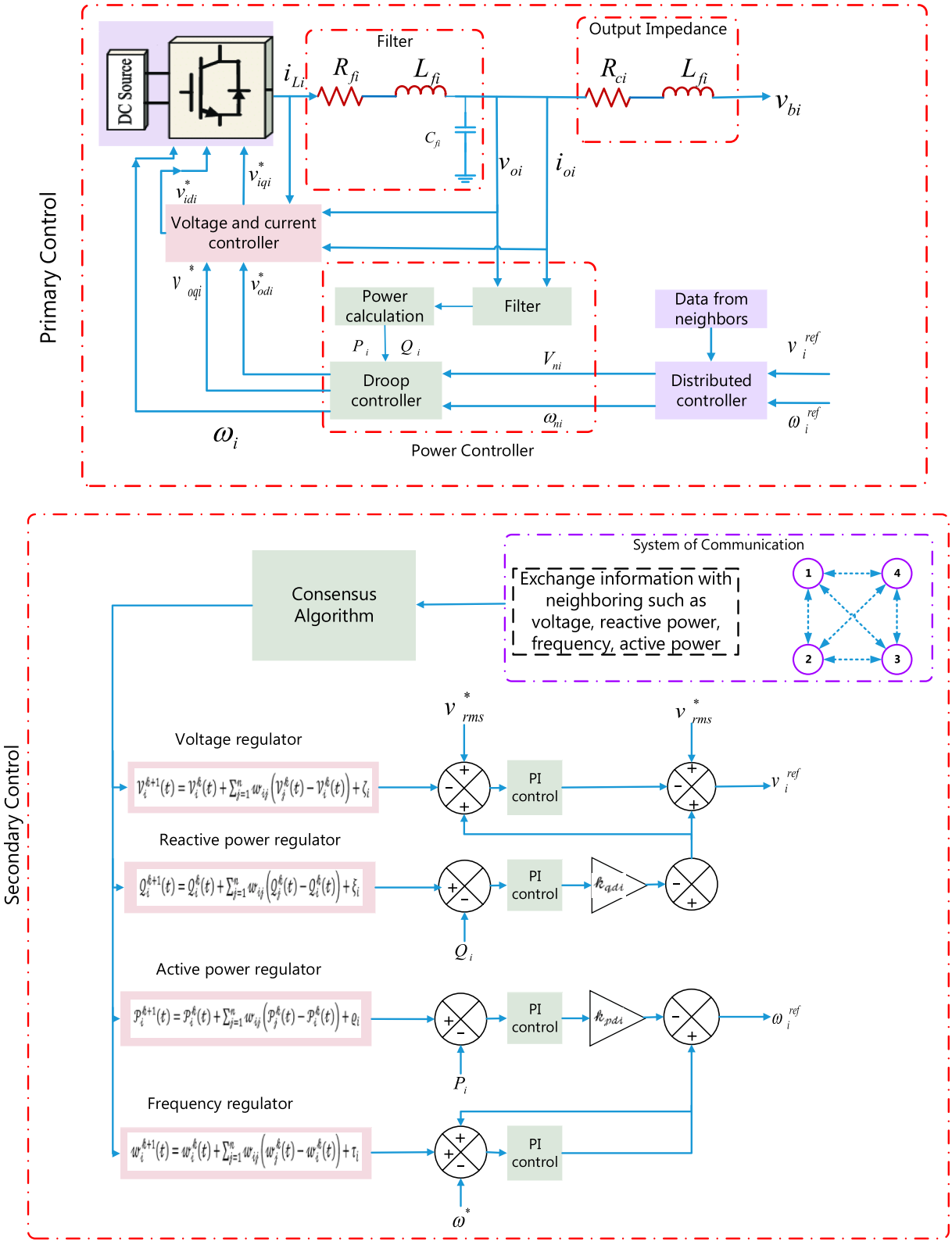

Fig. 1. Schematic diagram of the proposed FTC method in multi-agent MG.

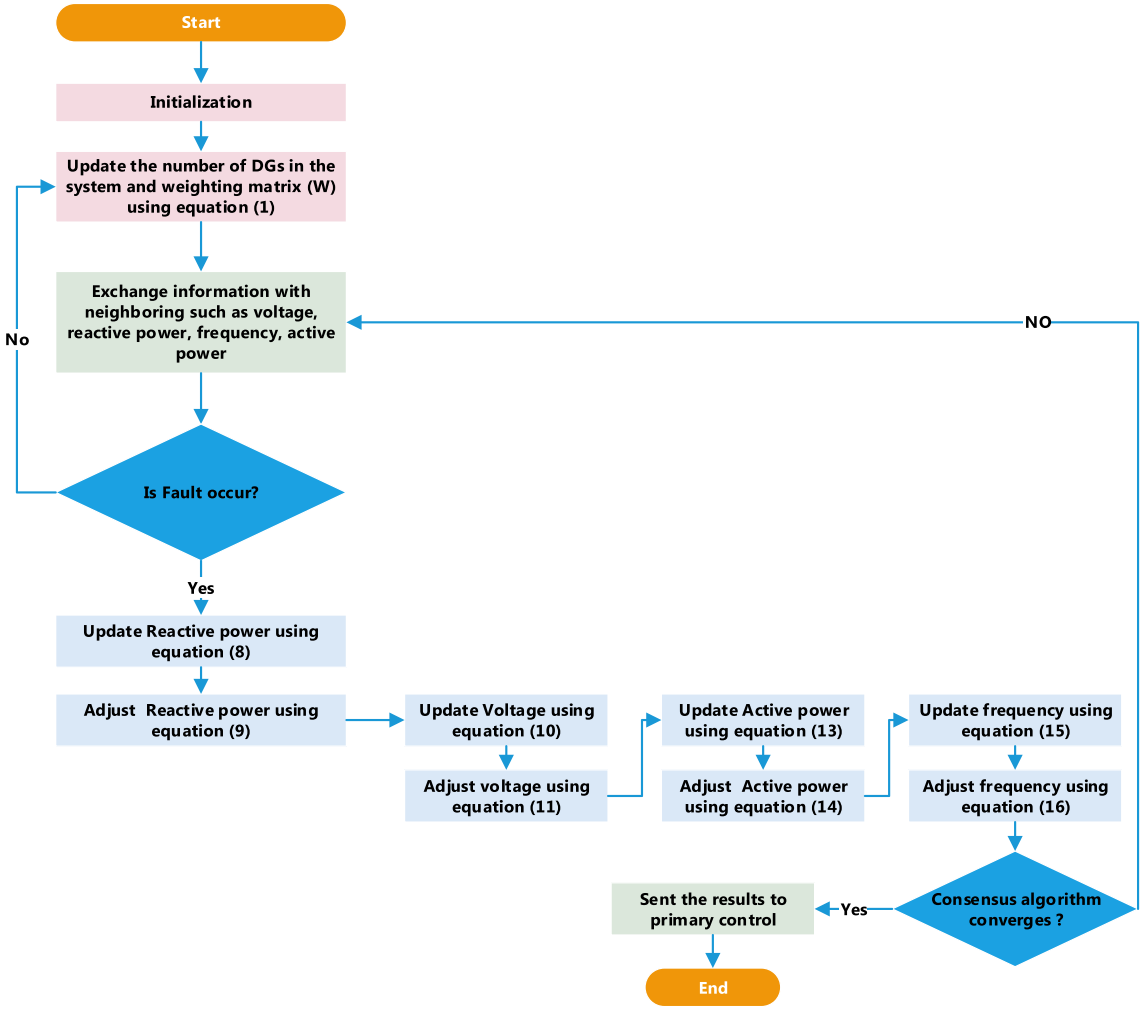

Fig. 2. The flowchart of the proposed corrective method.

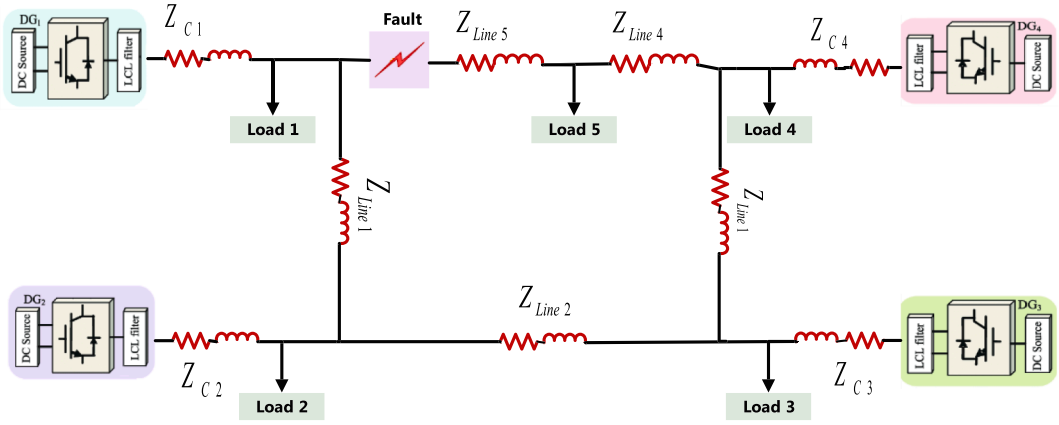

Fig. 3. Schematic single-line diagram of the MG.

compensation coefficient (13); also, the system frequency error is compensated according to (15). The angular frequency reference signal that has been sent to the primary DCM using the secondary consensus control method is represented as follows;

$$w_i^{ref} = w^* + \Im_{wi}^{k}(\ell) + k_{pdi}\Im_{Pi}^{k}(\ell) \quad (17)$$

The proposed control algorithms have been represented in Tables 2 and 3. The schematic diagram of the proposed FTC method for multi-agent MG has been shown in Fig. 1. The flowchart of the proposed controller has been introduced in Fig. 2.

Table 4
Parameters of MG test system.

DG 1 and 2			DG 3 and 4	
DGs	m_p	9.4×10^{-5}	m_p	12.5×10^{-5}
	n_Q	1.3×10^{-3}	n_Q	1.5×10^{-3}
	$L_{f1}, L_{f2},$	$1.35, 0.27\ mH$	$L_{f1}, L_{f2},$	$1.35, 0.27\ mH$
	$R_{f1}, R_{f2},$	$0.1, 0.05\ \Omega$	$R_{f1}, R_{f2},$	$0.1, 0.05\ \Omega$
	C_f	$47\ \mu F$	C_f	$47 \mu F$
	K_{PV}	0.1	K_{PV}	0.05
	K_{IV}	420	K_{IV}	390
	K_{PC}	15	K_{PC}	10.5
	K_{IC}	200,000	K_{IC}	160,000
	Z_c	$0.15 + j0.65\Omega$	Z_c	$0.3 + j0.65\Omega$
Lines	Z_{Line1}, Z_{Line4}	$0.12 + j0.1\Omega$	Z_{Line3}	$0.12 + j0.1\Omega$
	Z_{Line2}	$0.175 + j0.58\Omega$	Z_{Line5}	$0.175 + j0.58\Omega$
RL Loads	Load 1	$R = 300\Omega, L = 477\ mH$	Load 3	$R = 50\Omega, L = 64\ mH$
	Load 2 and Load 5	$R = 40\Omega, L = 64\ mH$	Load 4	$R = 50\Omega, L = 95\ mH$

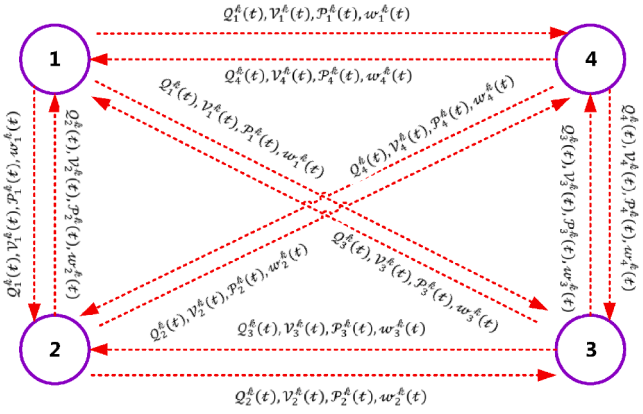

Fig. 4. The information exchange graph among the connected agents.

6. System modelling and simulation results

The proposed distributed secondary consensus-based FTC method is applied and verified using a hypothetical multi-agent MG system. Fig. 3 shows the schematic single-line diagram of the multi-agent MG test system, and Table 4 represents the parameters of the MG test system, including the load, DGs, and line parameters. A communication topology graph between the agents in MG is illustrated in Fig. 4. To prove the efficiency and the applicability of the proposed controller, different fault cases are applied to the MG test system;

(1) Case 1: three-line to ground fault (TL-G)
(2) Case 2: single line to ground fault (SL-G)
(3) Case 3: line to line fault (L-L)
(4) Case 4: double line to Ground (DL-G)

A comparison between the results obtained from applying the proposed secondary controller and the primary droop controller is performed. The proposed controller's performance is evaluated based on control system time response, maximum frequency deviation, and the steady-state restoration time. It is designed for all these cases that the fault occurs at t = 3 s, and the fault is cleared at t = 4 s.

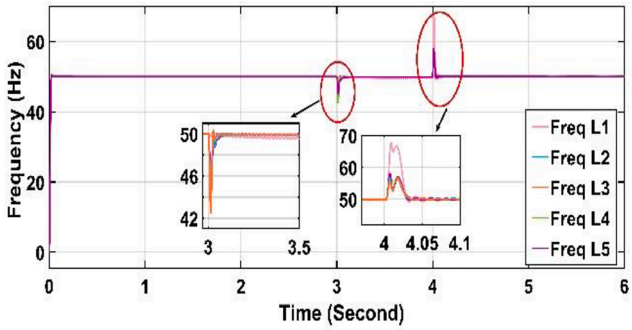

(a)

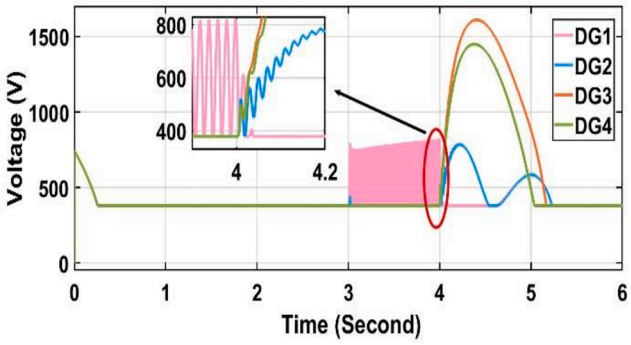

(b)

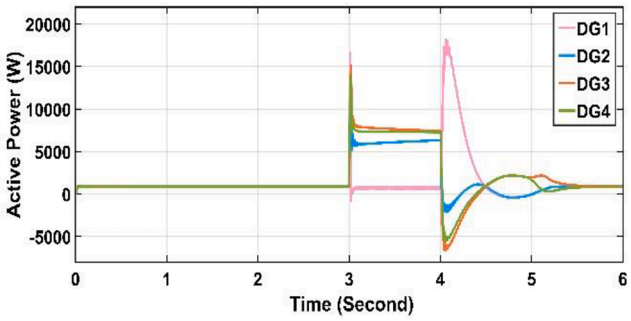

(c)

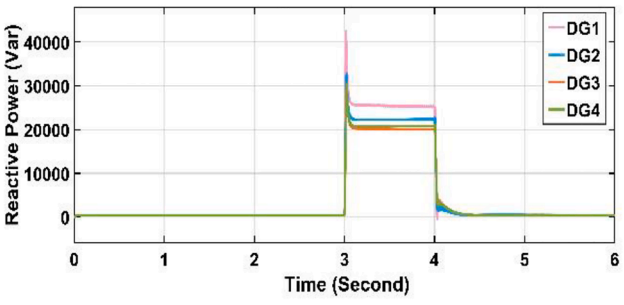

(d)

Fig. 5. Results of TL-G fault using the DCM (a) System frequency at each load bus, (b) Voltage at each DG bus, (c) Active power-sharing at each DG, (d) Reactive power-sharing at each DG.

(1) Case 1: three-line to ground fault

The proposed method is verified using the multi-agent MG system shown in Fig. 3. In this case, the TL-G fault occurs at load 1 and load 5.

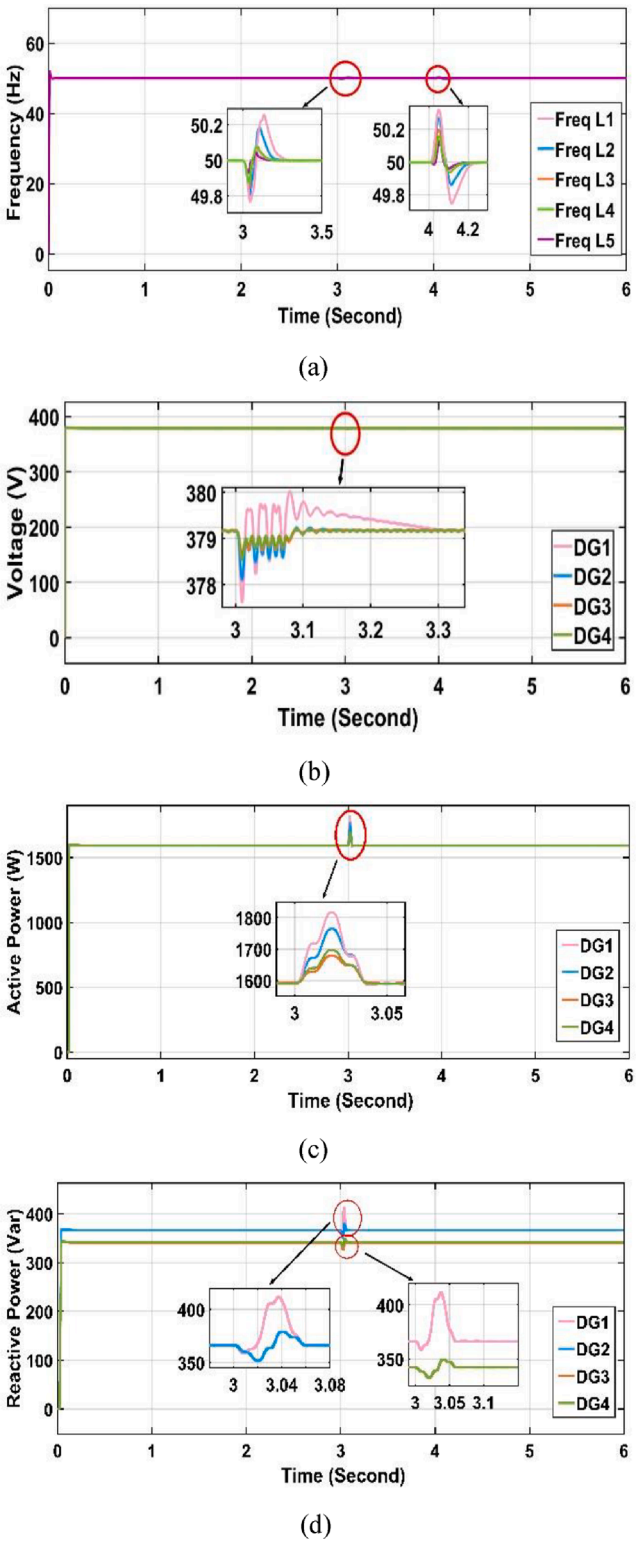

Fig. 6. Results of TL-G fault using the proposed method (a) System frequency at each load bus, (b) Voltage at each DG bus, (c) Active power-sharing at each DG, (d) Reactive power-sharing at each DG.

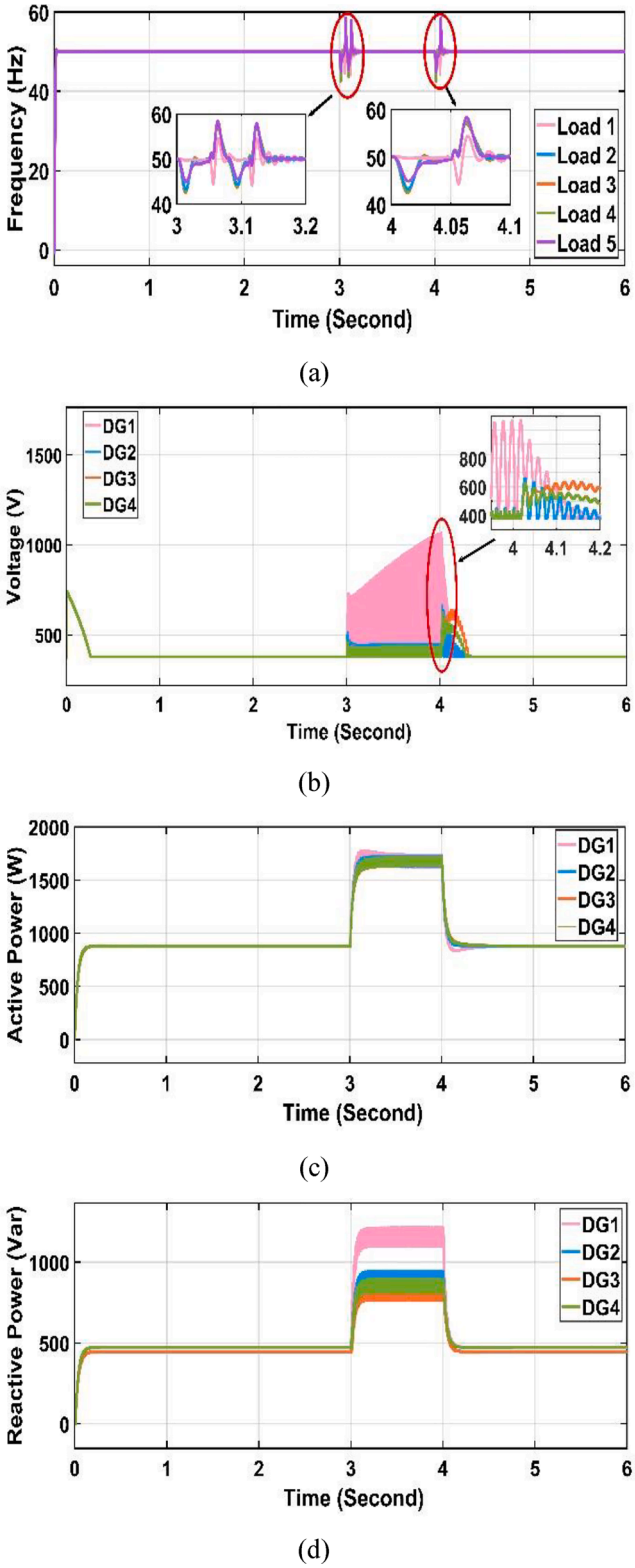

Fig. 7. Results of SL-G fault using the DCM (a) System frequency at each load bus, (b) Voltage at each DG bus, (c) Active power-sharing at each DG, (d) Reactive power-sharing at each DG.

The primary droop controller can't compensate for the MG-VF waveforms' errors, and there is an error in active and reactive power-sharing between the connected DGs in the MG. The proposed secondary consensus controller can transfer the system parameters' information as; voltage, frequency, active power, and reactive power from the neighbor agents through the communication network graph shown in Fig. 4. Hence, the MG-*VF* are restored to their nominal values, and the active and reactive power are shared equally among the connected DGs. Fig. 5 shows the system voltage, frequency, active power, and reactive power for each bus in the multi-agent MG by applying DCM. However, the

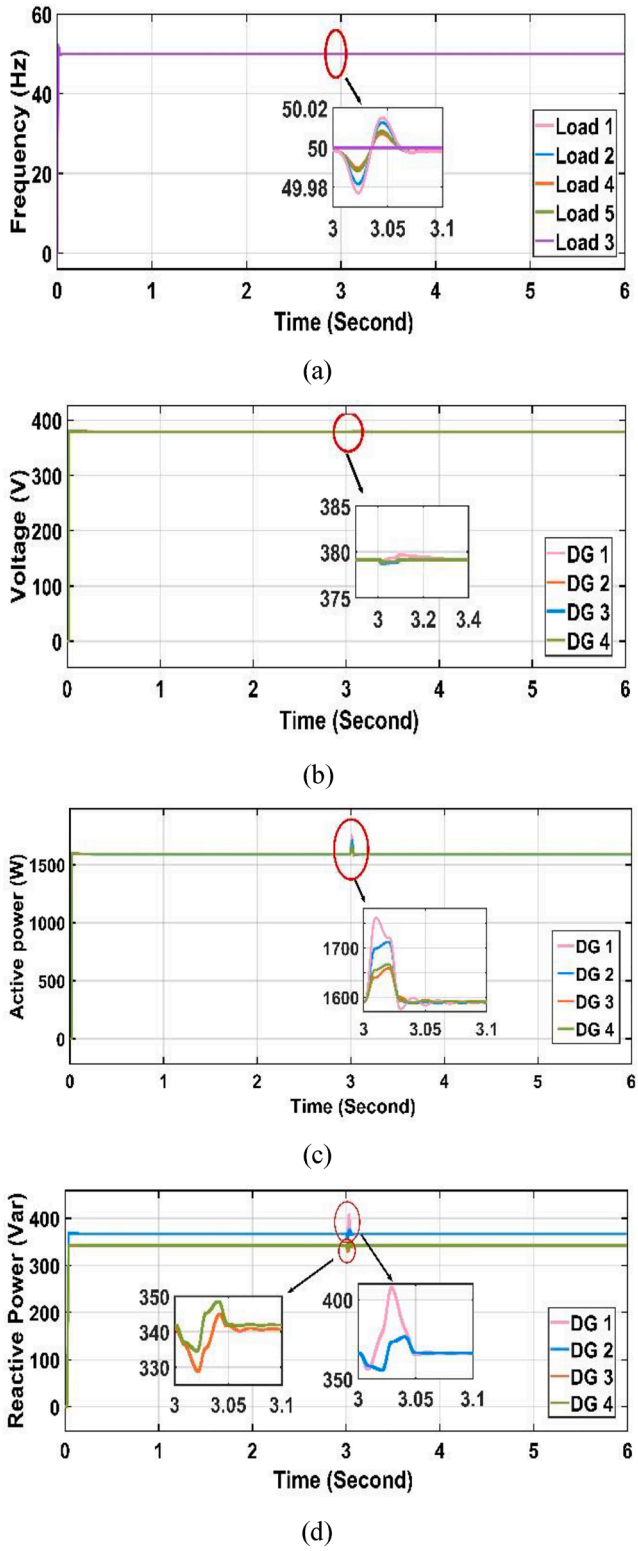

Fig. 8. Results of SL-G fault using the proposed method (a) System frequency at each load bus, (b) Voltage at each DG bus, (c) Active power-sharing at each DG, (d) Reactive power-sharing at each DG.

system voltage, frequency, and active and reactive power obtained after applying the proposed controller represented in Fig. 2 are shown in Fig. 6. By using the proposed secondary controller, the errors in the MG-*VF* waveforms are compensated, and the power is shared equally between the DGs in MG under the presence of three-line to ground fault.

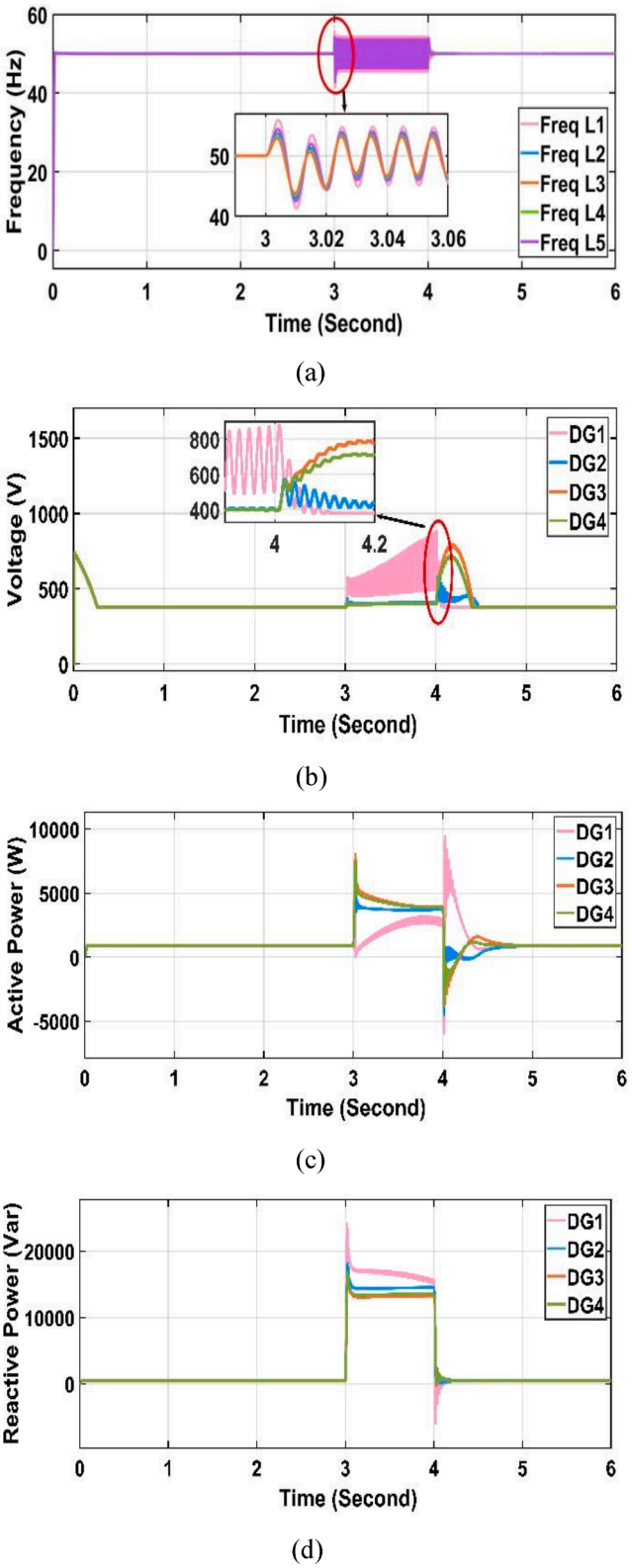

Fig. 9. Results of L-L fault using the DCM (a) System frequency at each load bus, (b) Voltage at each DG bus, (c) Active power-sharing at each DG, (d) Reactive power-sharing at each DG.

(2) **Case 2: single line to ground fault**

In this case, the proposed controller is verified using the multi-agent MG under the existence of a SL-G fault in the line between load 1 and

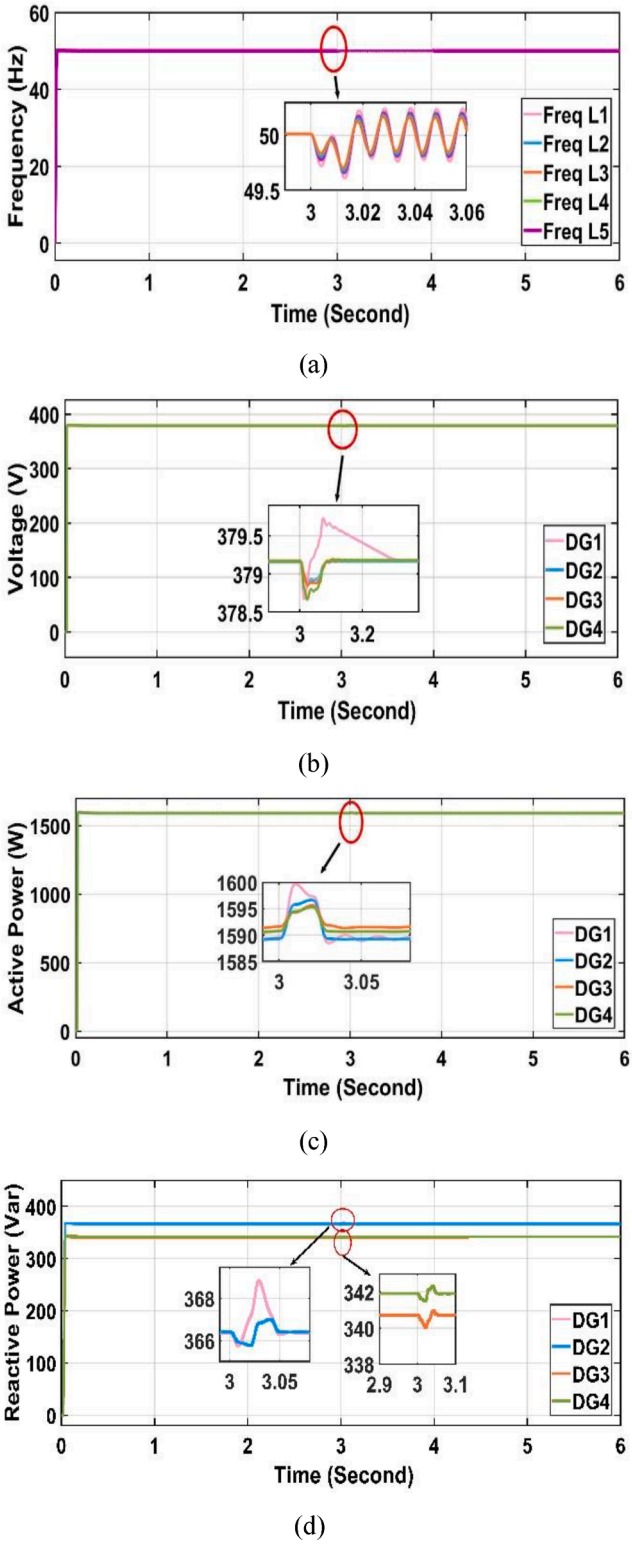

Fig. 10. Results of L-L fault using the proposed method (a) System frequency at each load bus, (b) Voltage at each DG bus, (c) Active power-sharing at each DG, (d) Reactive power-sharing at each DG.

load 5. Firstly, the droop controller is applied, and the output results of the system frequency, voltages, active power, and reactive power are shown in Fig. 7. Secondly, the proposed consensus secondary FTC method is applied, and Fig. 8 represents the obtained results of the frequency, voltages, active power, and reactive power.

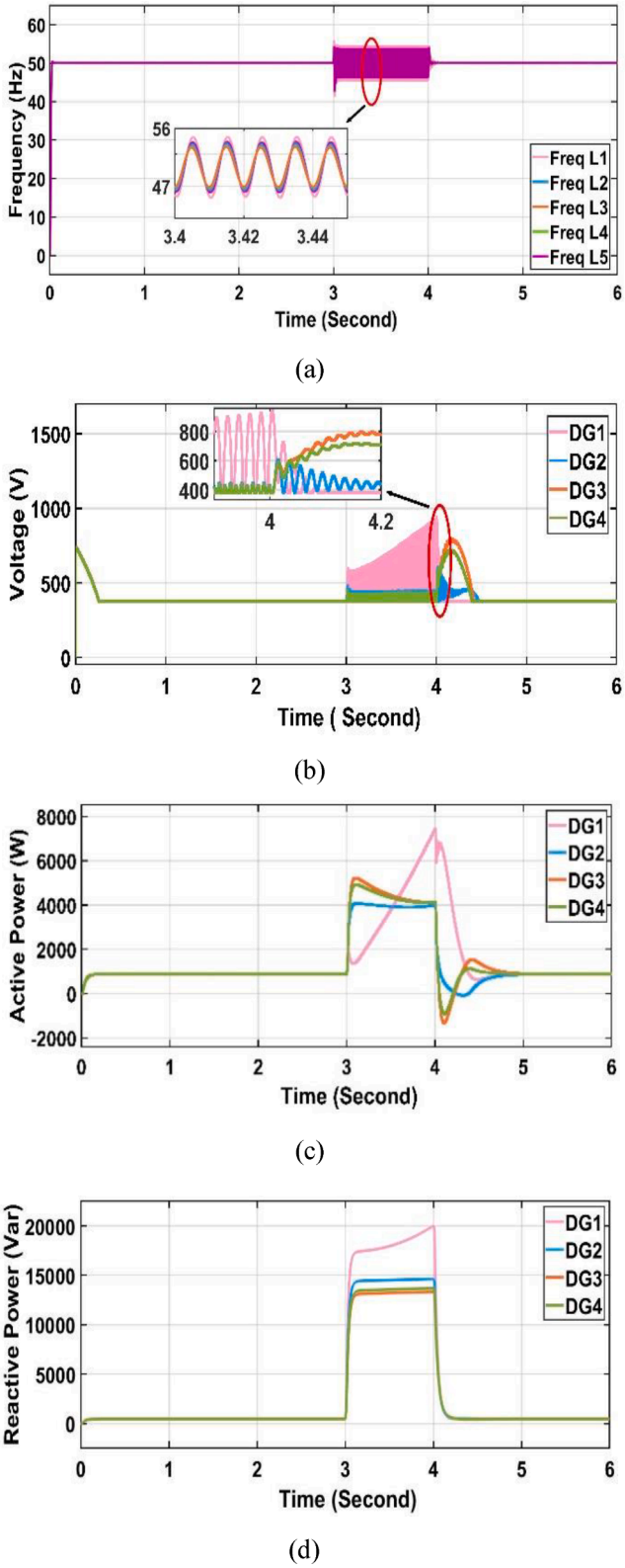

Fig. 11. Results of DL-G fault using the DCM (a) System frequency at each load bus, (b) Voltage at each DG bus, (c) Active power-sharing at each DG, (d) Reactive power-sharing at each DG.

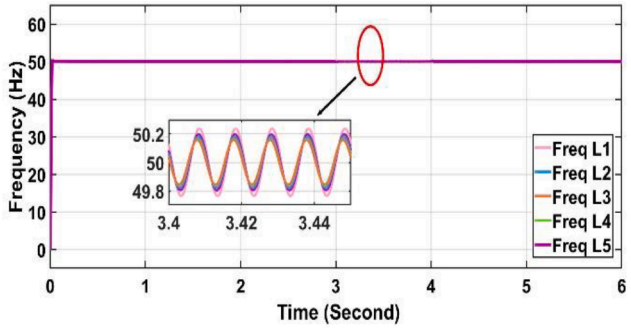

(a)

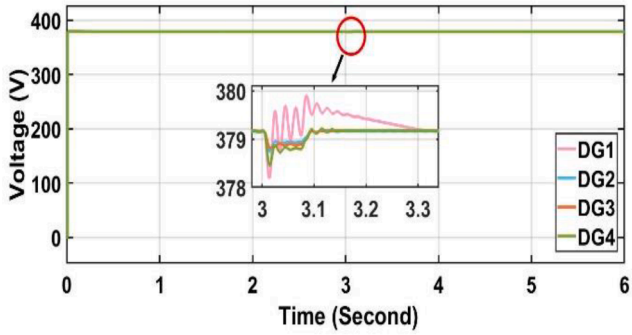

(b)

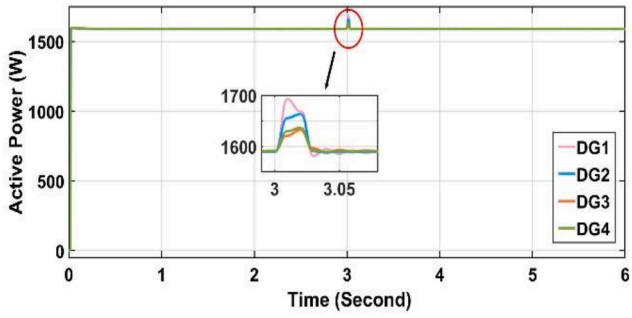

(c)

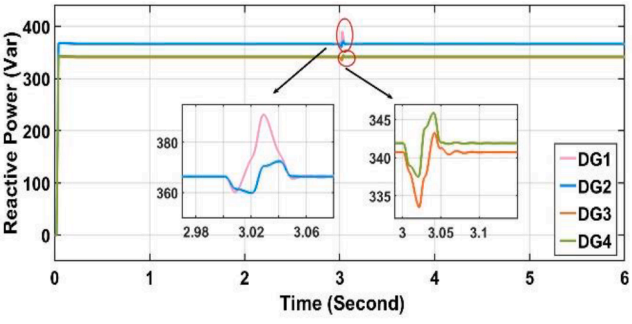

(d)

Fig. 12. Results of DL-G fault using the proposed method (a) System frequency at each load bus, (b) Voltage at each DG bus, (c) Active power-sharing at each DG, (d) Reactive power-sharing at each DG.

(3) Case 3: line to line fault

In this case, a L-L fault occurs in the line between load 1 and load 5. Fig. 9 shows the results obtained by applying conventional DCM. However, using the proposed controller, the MG-VF are adjusted to their nominal values, as shown in Fig. 10(a) and (b). The active and reactive power are also equally shared between the connected DGs, as represented in Fig. 10(c) and (d). The proposed secondary consensus control method enhances the MG resiliency in the presence of system faults.

(4) Case 4: double line to ground

A DL-G fault occurs in line between load 1 and load 5. Fig. 11 represents the results obtained by applying the DCM in the presence of the DL-G fault. Meanwhile, the results obtained by using the proposed controller are shown in Fig. 12. The proposed controller can eliminate the effects of the system fault that may occur in the multi-agent MG system.

7. Results analysis and discussion

This section analyzes the results obtained from applying the conventional DCM and the proposed secondary consensus controller. The main objective of the comparison between the two controllers is to prove the proposed controller's efficiency. This comparison is based on three indices, including the controller response time, the maximum frequency deviation, and the steady-state restoration time. The controller response time represents the proposed controller's ability to mitigate the effects of the system faults and restoring the MG-*VF* to their nominal values in a reasonable time. The maximum frequency deviation represents the proposed controller's ability to overcome the violation in the frequency waveform in the presence of the system fault. The steady-state restoration time represents the proposed controller's ability to restore the steady-state operation at a reasonable time.

Fig. 13 shows a comparison between the FTC based droop control and the proposed method according to the controller response time for the four connected bus bars. This comparison is performed under the presence of different fault conditions. By applying the proposed controller, the controller response time is improved by 0.33% for the TL-G fault, 0.66% for the SL-G fault, 0.33% for the L-L fault, and 0.49% for the DL-G fault at the four connected buses. A comparison between the droop controller and the proposed control method concerning the maximum frequency deviation is illustrated in Fig. 14. The maximum frequency deviation has been reduced by applying the proposed method by 98.22%, 96.49%, 97.28%, and 96.66% for the four connected buses, respectively, under the presence of the TL-G fault. Also, the improvement in the maximum frequency deviation for the four connected buses is 99.76%, 99.79%, 99.93%, and 99.86%, corresponding to the SL-G fault, 95.34%, 94.93%, 94.63%, and 94.26% considering the L-L fault, and 97.47%, 97.50%, 97.63%, and 97.74% in the presence of the DL-G fault. Fig. 15 shows the comparison between the droop and proposed control methods concerning the steady-state restoration time. By applying the proposed method, the system stability is preserved in a reasonable time. Under the TL-G fault, the steady-state restoration time is reduced by 45.71%, 45.32%, 45.51%, and 45.61% for the system's four buses. The steady-state restoration time is improved for the four buses by 33.11%, 32.96%, 33.11%, and 33.11% in the presence of the SL-G fault, 35.03%, 34.89%, 35.16%, and 35.30% with considering the L-L fault, and 37.65% in the presence of the DL-G for the four buses.

For the sake of comparison and verification, a comparison between the proposed controller and the neural sliding mode controller [6], MPC method [19], and H∞ controller [21]. The results are obtained for the four-fault conditions, TL-G fault, SL-G fault, L-L fault, and DL-G fault. Figs. 16–19 show the frequency and voltage waveforms for the four different fault conditions by applying the neural sliding mode controller [6], MPC [19], H∞ controller [21], and the proposed method at bus 1 for the system shown in Fig. 3. The fault occurs at 3 s, and the fault clearance at 4 s.

A comparison between the proposed controller and the neural sliding mode controller [6], MPC [19], and H∞ controller [21] is performed based on the controller response time, maximum frequency deviation,

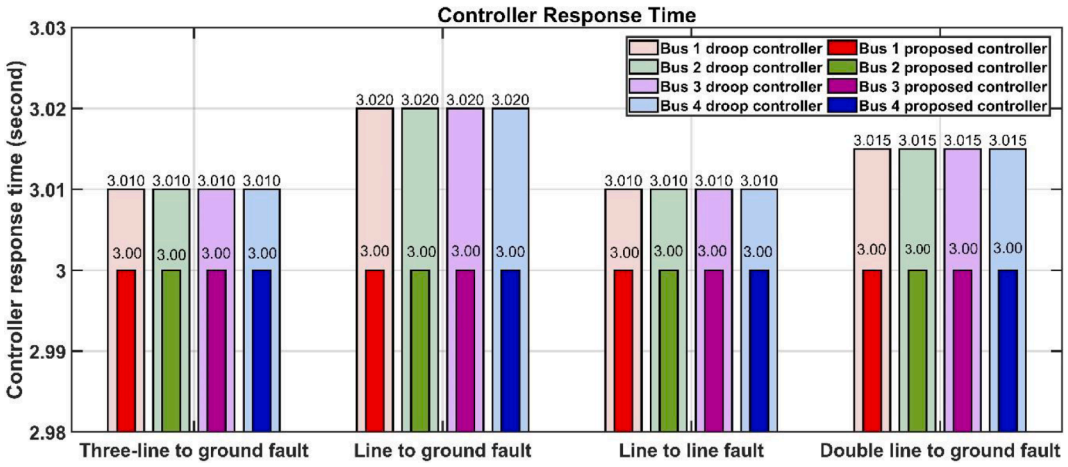

Fig. 13. Comparison between the droop controller and the proposed control methods-based controller response time.

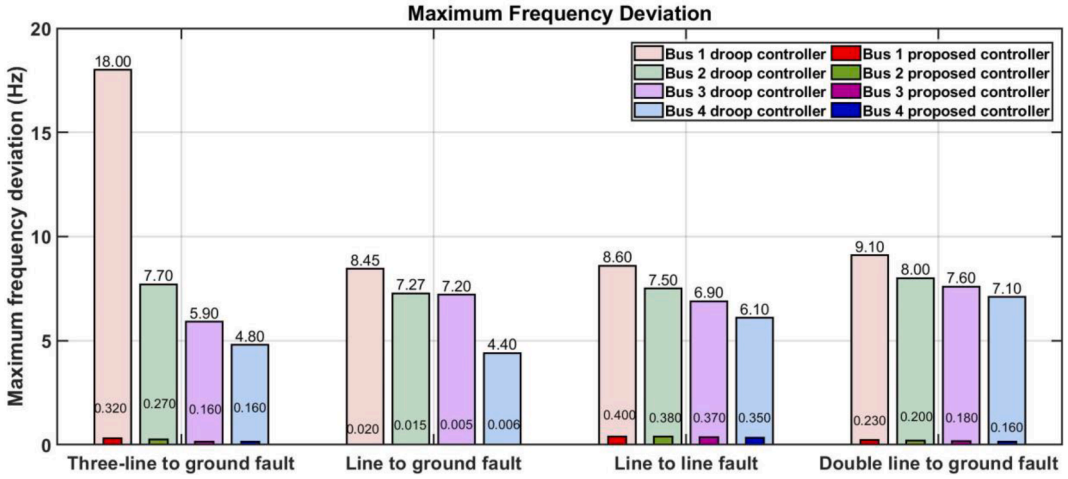

Fig. 14. Comparison between the droop controller and the proposed control methods-based maximum frequency deviation.

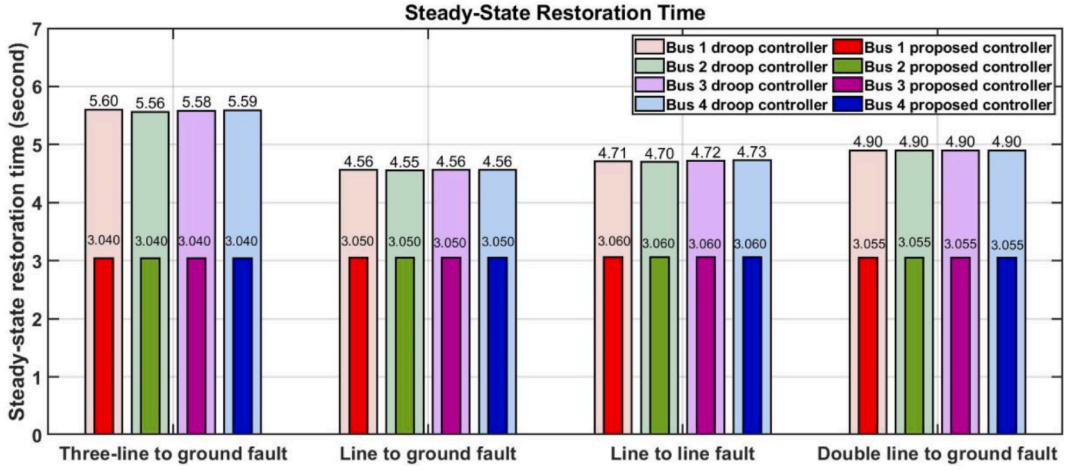

Fig. 15. Comparison between the droop controller and the proposed control methods-based steady-state restoration time.

and the steady-state restoration time concerning the droop controller. It can be observed that the controller response time does not improve in the presence of the different fault conditions with applying the neural sliding mode controller [6], MPC [19], and H∞ controller [21]. However, using the proposed method, the controller response time is improved for all different fault conditions, as shown in Fig. 20. The maximum frequency deviation is enhanced by applying the proposed controller over the other control methods presented in [6,19], and [21],

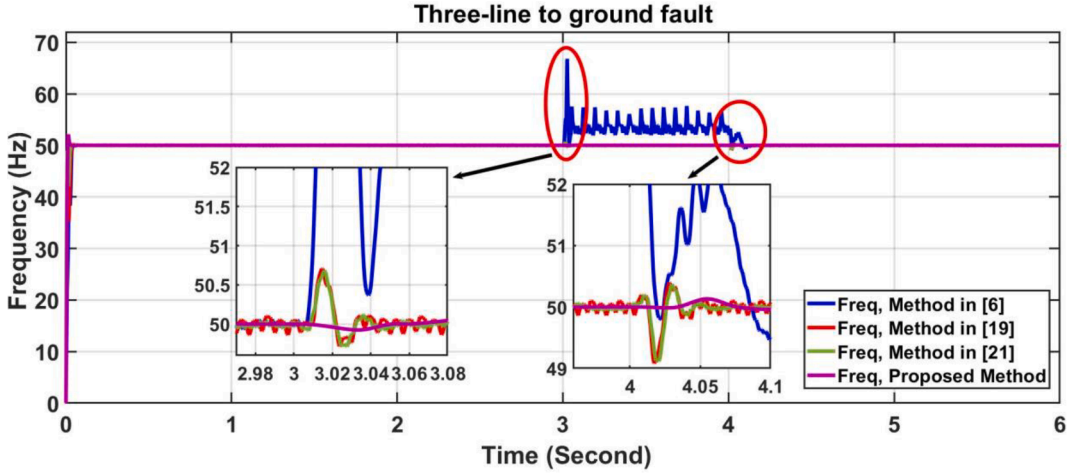

(a)

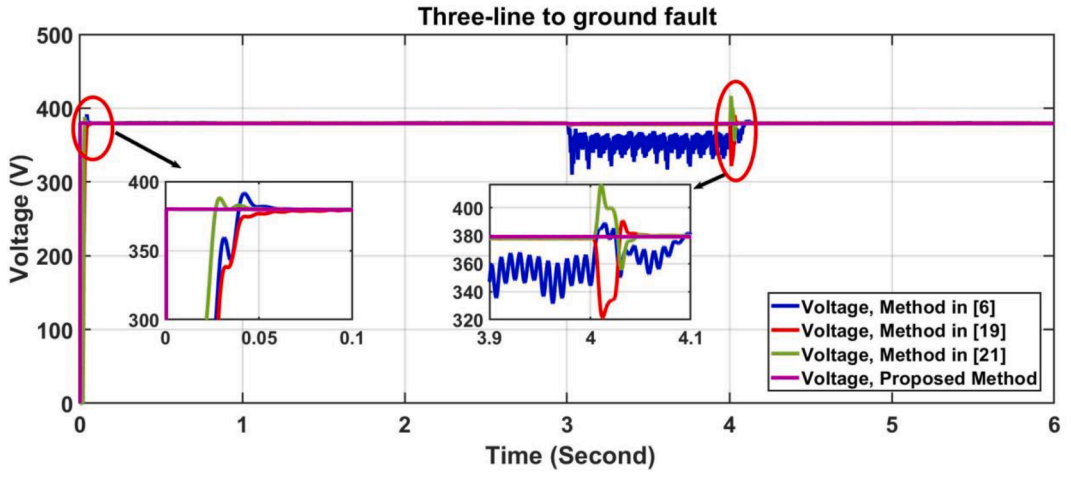

(b)

Fig. 16. Comparison between the proposed controller and the different controllers in the presence of three-line to ground fault (a) System frequency, (b) System voltage.

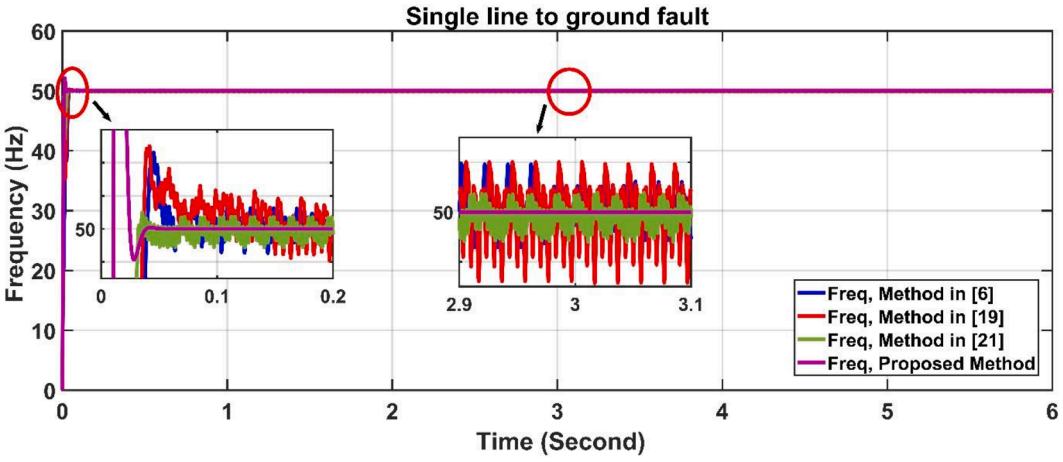

(a)

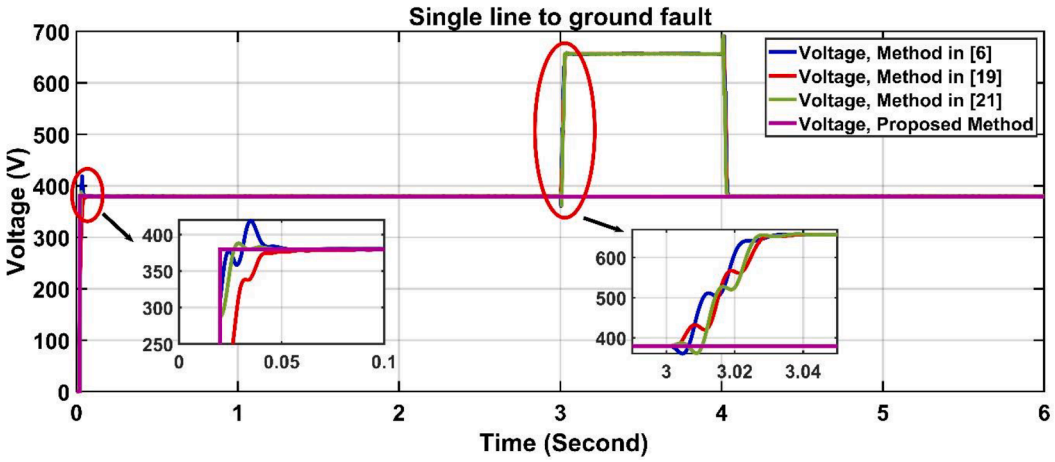

(b)

Fig. 17. Comparison between the proposed controller and the different controllers in the presence of line to ground fault (a) System frequency, (b) System voltage.

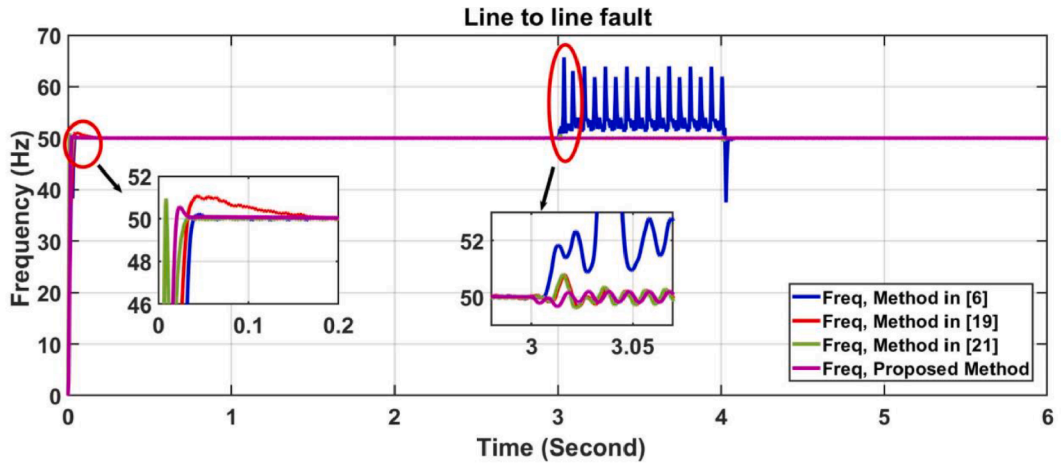

(a)

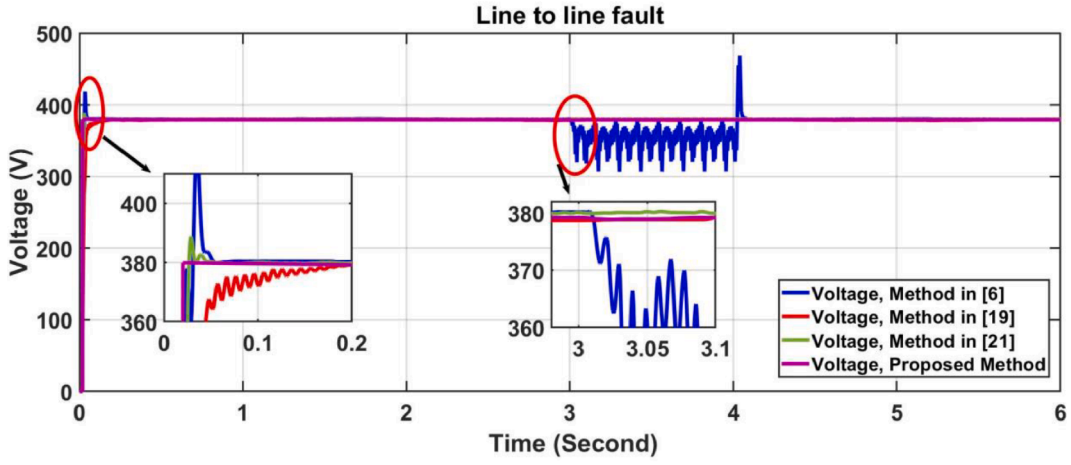

(b)

Fig. 18. Comparison between the proposed controller and the different controllers in the presence of line to line fault (a) System frequency, (b) System voltage.

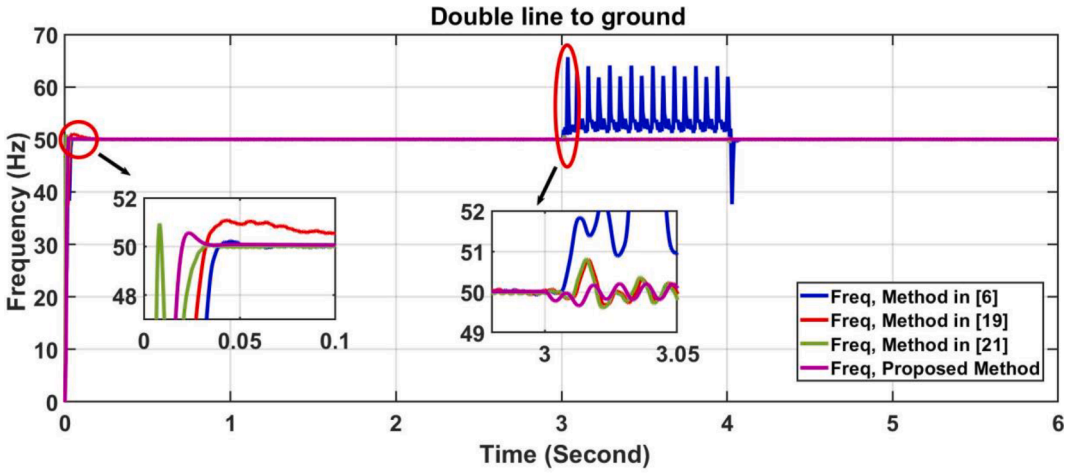

(a)

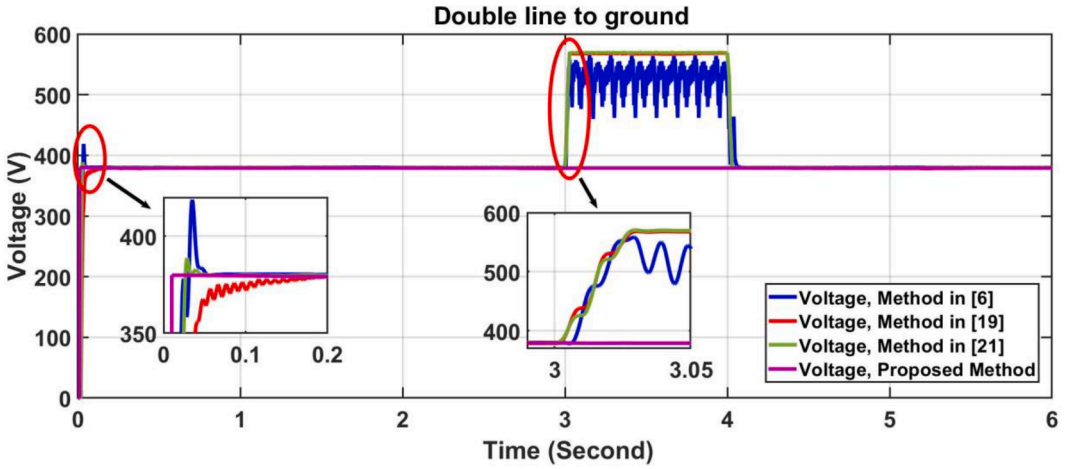

(b)

Fig. 19. Comparison between the proposed controller and the different controllers in the presence of double line to ground fault (a) System frequency, (b) System voltage.

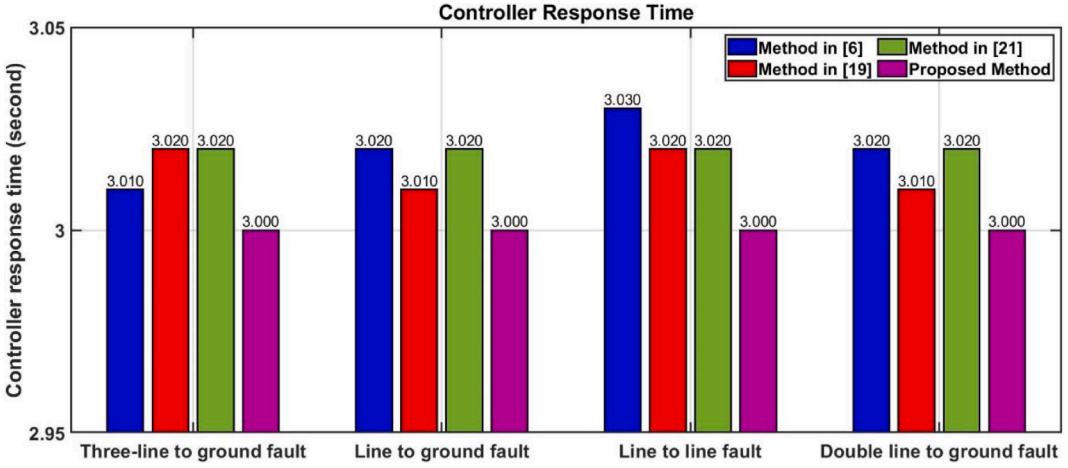

Fig. 20. Comparison between sliding-mode controller [6], model predictive control [19], adaptive H-infinity [21], and proposed control method-based on controller response time.

as shown in Fig. 21. Besides, Fig. 22 indicates that the proposed controller can restore the system's steady-state stability in a reasonable time compared to the control methods presented in [6,19], and [21].

The proposed distributed secondary consensus FTC method can restore the MG-VF and, optimally share the active and reactive power. It can overcome the faults' effect, and the controller responds to the

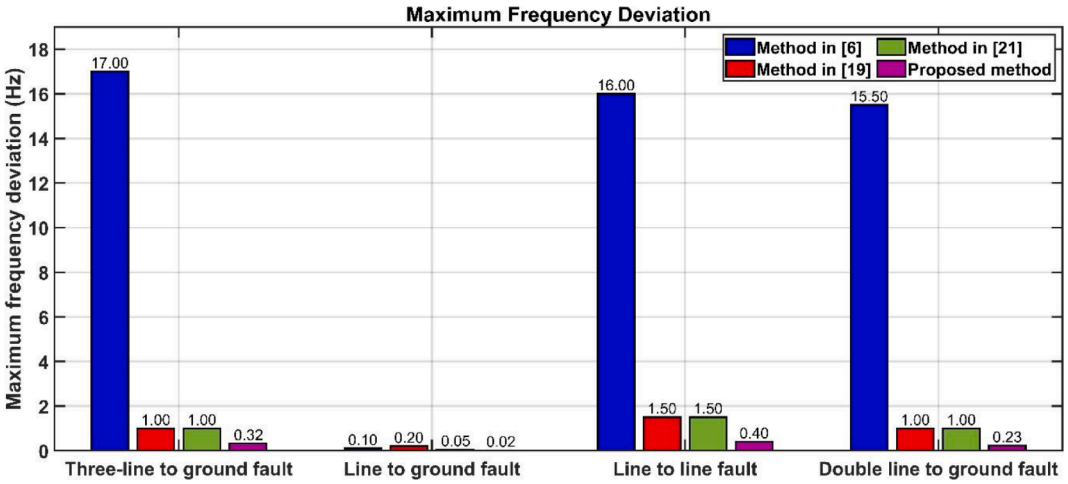

Fig. 21. Comparison between the sliding-mode controller [6], model predictive control [19], adaptive H-infinity [21], and proposed control methods-based on maximum frequency deviation.

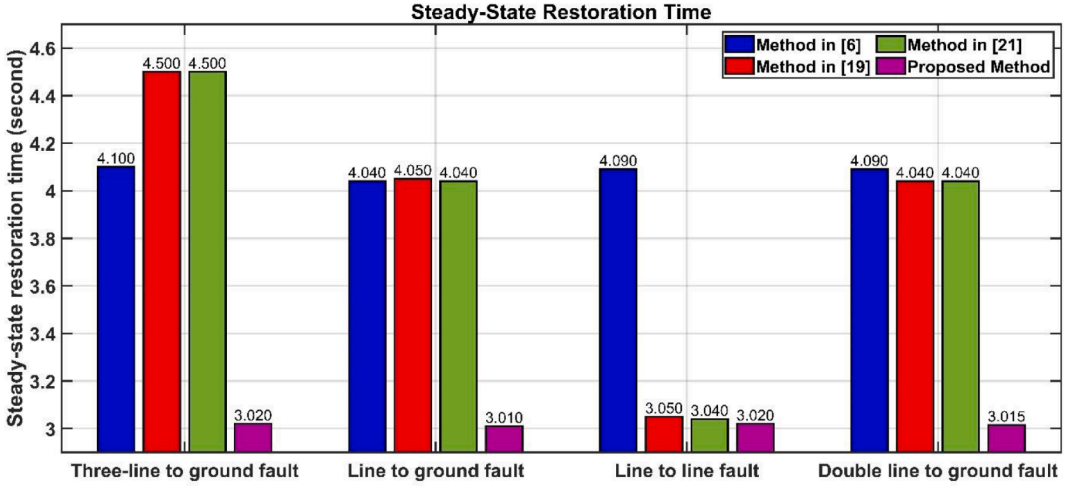

Fig. 22. Comparison between the sliding-mode controller [6], model predictive control [19], adaptive H-infinity [21], and proposed control methods-based on steady-state restoration time.

system faults and restore the steady-state system operation at a minimum time rather than the droop controller. The maximum frequency deviation is improved by applying the proposed controller as the controller response speed to the system faults prevents the frequency waveform from violating its nominal value. Using the proposed controller, the steady-state operation is reached in minimum time after the clearance of the system fault compared with the droop controller. In general, the proposed controller's performance is verified, and the results showed its effectiveness in tackling the effects of the system faults in the multi-agent MG while regulating the MG-*VF* and enhancing the active and reactive power -allocation between the connected DGs.

8. Conclusion

This paper proposed a distributed secondary consensus-based FTC method to mitigate the transmission system faults' impacts in the multi-agents MG. The proposed consensus controller depends on the information transferring between the connected agents in the MG system. The errors in frequency and voltage waveforms have been compensated by applying the proposed consensus controller, and also, the active and reactive power are optimally shared among the DGs. The proposed controller improves the performance of the primary DCM that can't adjust the MG-*VF* to their nominal values, and also, it doesn't enhance the power-sharing among the DGs in MG. A hypothetical multi-agent MG system is designed to prove the proposed controller's effectiveness using the MATLAB/Simulink environment in the presence of the different short-circuit faults in the transmission line in MG. A comparative analysis between the proposed controller and the DCM is established based on controller response time, the maximum frequency deviation, and the steady-state restoration time. The obtained results have shown that the proposed controller regulates MG's frequency and voltage under different faults. Active and reactive power are equally shared between the DGs. For the sake of verification, the efficacy of the proposed method is compared with the droop controller, neural sliding mode controller, MPC method, and H∞ controller. The obtained results prove that the proposed control method has a fast response to the fault occurrence, reduces frequency deviation, and achieves steady-state operation with a reasonable time than the other control methods.

Declaration of Competing Interest

The authors declare that they have no known competing financial interests or personal relationships that could have appeared to influence the work reported in this paper.

Appendix A

A comparison between the different control methods based on pros and cons is performed (see Table 5).

Table 5
Comparison between different control methods [39–46].

Method	Pros	Cons
Multi-agent system control	■ Intelligence guaranteed and cost minimization ■ Proactive and social adaptability ■ Effective in a microgrid with a large number of RESs ■ Applicable for both grid-connected and islanded modes ■ Simpler and improve the system reliability ■ Decides whether an MG connected load has to consume power from an agent or not	■ Rely on communication ■ Sensitive to a communication failure ■ Signal transmission delays
Sliding mode control	■ Lowest error and good disturbance rejection ■ Low computational burden and do not require mathematical data ■ Soften the control signal ■ Applicable for both grid-connected and islanded modes ■ Reliable performance during transient ■ Control the power quality based on design ■ Ensure the stability of the constrained parameters for robust nonlinear control ■ It has robustness versus the disturbance and the model uncertainties ■ Applicable for the nonlinear controller	■ Complex and low speed ■ Chattering phenomena in discrete implementation ■ Difficult in designing procedure ■ Proper transient and zero steady-state error ■ Not robust to accommodate load variations
Reinforcement learning algorithm	■ Can determine optimal policy decisionv ■ Provides a robust system performance ■ Conducts learning without prior knowledge ■ Can solve the continuous state space control problems ■ Highly scalable	■ A finite set of state and action called the Markov decision process ■ Long-time convergence for a large real-world problem if not good initialization ■ The action-value function is challenging to model ■ Policy training time is long
Model predictive control	■ Explicit consideration of constraints ■ Easy to tune ■ Handling of multivariable control problems ■ Applicable for both grid-connected and islanded modes ■ Robust against uncertainties ■ Suitable for use in nonlinear system ■ Require less switching frequency ■ Fast dynamic response ■ The most popular control method in the industry ■ Fast computing and economical method ■ Predict dynamic system behavior over a finite horizon ■ Its straightforward applicability to large and multivariable processes	■ It cannot tune offline ■ It cannot be used in uncertain systems and cannot deal with unknown parameters ■ Frequency response nature cannot be visualized ■ Require accurate filter model ■ Sensitive to the network parameter ■ High computational requirement ■ Cannot correctly recognize the process model ■ Performance analysis is quite difficult
H-infinity (H∞)	■ Robust performance in linear, nonlinear, and unbalanced loads ■ Reduced tracking error ■ Synthesize the system stability ■ Improve the system performance in the presence of parameters uncertainty and external disturbances ■ Enhancing the transient stability under the presence of uncertainties ■ Repetitive control ■ Improve the system power quality ■ Used for multi-input multi-output (MIMO) models ■ Can minimize the effect of perturbations on the control system ■ Handle fixed and random delay	■ Require deep mathematical understanding ■ Relatively slow dynamics ■ Impractical for large system dimensions and with no constraints handling ■ Large computation ■ Complex algorithm
Consensus control	■ Scalability, extendibility, and modularity ■ Applicable for both grid-connected and islanded modes ■ Improved negative sequence current sharing under unbalanced loading ■ Support plug and play capability ■ Improve the load current sharing accuracy ■ Increase flexibility and enhance redundancy ■ Uses low bandwidth communication ■ Capable of handling uncertain and disturbances ■ Decentralized data updating ■ Faster decision-making method and action ■ Increase computational efficiency ■ Guaranteed frequency restoration ■ Guaranteed proportional active power-sharing ■ Robust to system parameter variations and communication configuration changes ■ Adaptive to various operating conditions ■ Guaranteed smooth transient process	■ Communication-based ■ Costly and time-consuming ■ Sensitive to a communication failure ■ Signal transmission delays ■ The coordination and synchronization method necessitates the exchange of data among agents based on particular communication protocols

References

[1] Chen L, Wang Y, Lu X, Zheng T, Wang J, Mei S. Resilient active power sharing in autonomous microgrids using pinning-consensus-based distributed control. IEEE Trans Smart Grid 2019;10(2):6802–11.
[2] Sedhom B, El-Saadawi M, Hatata A, Alsayyari A. Hierarchical control technique-based harmony search optimization algorithm versus model predictive control for autonomous smart microgrids. Int J Electr Power Energy Syst 2020;115:105511.
[3] Yoo H, Nguyen T, Kim H. Consensus-based distributed coordination control of hybrid AC/DC microgrids. IEEE Trans Sustain Energy 2019;11(2):629–39.
[4] Zhang F, Mu L. A fault detection method of microgrids with grid-connected inverter interfaced distributed generators based on the PQ control strategy. IEEE Trans Smart Grid 2019;10(5):4816–26.
[5] Shahab M, Mozafari B, Soleymani S, Dehkordi N, Shourkaei H, Guerrero J. Distributed consensus-based fault tolerant control of islanded microgrids. IEEE Trans Smart Grid 2020;11(1):37–47.
[6] Djilali L, Sanchez E, Tellez F, Avalos A, Belkheiri M. Improving microgrid low-voltage ride-through capacity using neural control. IEEE Syst J 2020;14(2):2825–36.
[7] Sahoo S, Kishore N, Sinha A. Decentralised control and fault ride-through of a multi-microgrid system. IET Smart Grid 2019;2(3):464–76.
[8] Ahumada C, Crdenas R, Sez D, Guerrero J. Secondary control strategies for frequency restoration in islanded microgrids with consideration of communication delays. IEEE Trans Smart Grid 2016;7(3):1430–41.
[9] Cai H, Hu G, Lewis F, Davoudi A. A distributed feedforward approach to cooperative control of AC microgrids. IEEE Trans Power Syst 2016;31(5):4057–67.
[10] Schiffer J, Seel T, Raisch J, Sezi T. Voltage stability and reactive power sharing in inverter-based microgrids with consensus based distributed voltage control. IEEE Trans Control Syst Technol 2016;24(1):96–109.
[11] Dehkordi N, Sadati N, Hamzeh M. Distributed robust finite time secondary voltage and frequency control of islanded microgrids. IEEE Trans Power Syst 2017;32(5):3648–59.
[12] Bintoudi A, Zyglakis L, Tsolakis A, Loannidis D, Hadjidemetriou L, Zacharia L, et al. Hybrid multi-agent-based adaptive control scheme for AC microgrids with increased fault-tolerance needs. IET Renew Power Gener 2020;14(1):13–26.
[13] Bintoudi A, Zyglakis L, Tsolakis A, Ioannidis D, Hadjidemetriou L, Zacharia L, et al. A hybrid multi-agent-based adaptive control scheme for AC microgrids with increased fault-tolerance needs. IET Renew Power Gener 2020;14(1):13–26.
[14] Morshed M, Fekih A. A fault-tolerant control paradigm for microgrid-connected wind energy systems. IEEE Syst J 2018;12(1):360–72.
[15] Liu C, Jiang B, Patton R, Zhang K. Decentralized output sliding-mode fault-tolerant control for heterogeneous multiagent systems. IEEE Trans Cybern 2020;50(12):4934–45.
[16] Li H, Wu Y, Chen M. Adaptive fault-tolerant tracking control for discrete-time multiagent systems via reinforcement learning algorithm. IEEE Trans Cybern 2021;51(3):1163–74.
[17] Younesi A, Shayeghi H, Siano P. Assessing the use of reinforcement learning for integrated voltage/frequency control in AC microgrids. Energies 2020; 13(5).
[18] Morato M, Mendes P, Rico J, Bordons C. LPV-MPC fault-tolerant energy management strategy for renewable microgrids. Int J Electric Power Energy 2020;117:105644.
[19] Wei Juan, Li Canbing, Wu Qiuwei, Zhou Bin, Xu Da, Huang Sheng. MPC-based DC-link voltage control for enhanced high-voltage ride-through of offshore DFIG wind turbine. Int J Electr Power Energy Syst 2021;126:106591.
[20] Bernardi E, Morato M, Mendes P, Normey-Rico J, Adam E. Fault-tolerant energy management for an industrial microgrid: A compact optimization method. Int J Electr Power Energy Syst 2021;124:106342.
[21] Sedhom Bishoy E, Hatata Ahmed Y, El-Saadawi Magdi M, Abd-Raboh El-Hosaini E. Robust adaptive H-infinity based controller for islanded microgrid supplying nonlinear and unbalanced loads. IET Smart Grid 2019;2(3):420–35.
[22] Afshari A, Karrari M, Baghaee H, Gharehpetian G. Distributed fault-tolerant voltage/frequency synchronization in autonomous AC microgrids. IEEE Trans Power Syst 2020;35(5):3774–89.
[23] Afshari A, Karrari M, Baghaee H, Gharehpetian G, Karrari S. Cooperative fault-tolerant control of microgrids under switching communication topology. IEEE Trans Smart Grid 2020;11(3):1866–79.
[24] Jin X, Zhao X, Wu X, Chi J. Adaptive fault tolerant consensus for a class of leader-following systems using neural network learning strategy. Neural Networks 2020;121:474–83.
[25] Duan J, Yuen M. Robust consensus-based distributed energy management for microgrids with packet losses tolerance. IEEE Trans Smart Grid 2020;11(1):281–90.
[26] Molzahn D, Dorfler F, Sandberg H, Low S, Chakrabarti S, Member S, et al. A survey of distributed optimization and control algorithms for electric power systems. IEEE Trans Smart Grid 2017;8(6):2941–62.
[27] Yu L, Shi D, Xu G, Guo X, Jiang Z, Jing G. Consensus control of distributed energy resources in a multi-bus microgrid for reactive power sharing and voltage control. Energies 2018; 11(10).
[28] Dehkordi N, Moussavi S. Distributed resilient adaptive control of islanded microgrids under sensor/actuator faults. IEEE Trans Smart Grid 2019;11(3):2699–708.
[29] Li X, Xu Q, Blaabjerg F. Adaptive resilient secondary control for islanded AC microgrids with sensor faults. IEEE J Emerg Selected Topics Power Electron 2020. https://doi.org/10.1109/JESTPE.2020.2988509.
[30] Zhang B, Dou C, Yue D, Zhang Z, Zhang T. Hierarchical control strategy for networked DC microgrid based on adaptive dynamic program and event-triggered consensus algorithm considering economy and actuator fault. J Franklin Inst 2020;357(13):8631–56.
[31] Jin X, Zhao X, Yu J, Wu X, Chi J. Adaptive fault-tolerant consensus for a class of leader-following systems using neural network learning strategy. Neural Networks 2020;121:474–83.
[32] Lai J, Lu X, Tang R, Li X, Dong Z. Delay-tolerant distributed voltage control for multiple smart loads in AC microgrids. ISA Trans 2019;86:181–91.
[33] Qin J, Zhang G, Zheng WX, Kang Y. Adaptive sliding mode consensus tracking for second-order nonlinear multiagent systems with actuator faults. IEEE Trans Cybern 2019;49(5):1605–15.
[34] Ye D, Zhao X, Cao B. Distributed adaptive fault-tolerant consensus tracking of multi-agent systems against time-varying actuator faults. IET Control Theory Appl 2016;10(5):554–63.
[35] Ma H, Yang G. Adaptive Fault Tolerant Control of Cooperative Heterogeneous Systems with Actuator Faults and Unreliable Interconnections. IEEE Trans Autom Control 2016;61(11):3240–55.
[36] Wang Y, Song Y, Lewis FL. Robust adaptive fault-tolerant control of multiagent systems with uncertain nonidentical dynamics and undetectable actuation failures. IEEE Trans Ind Electron 2015;62(6):3978–88.
[37] Sahoo S, Peng J, Annavaram D, Mishra S, Dragicevic T. On Detection of false data in cooperative DC Microgrids-A discordant element approach. IEEE Trans Ind Electron 2020;67(8):6562–71.
[38] Sedhom B, El-Saadawi M, Elhosseini M, Saeed M, Abd-Raboh E. A harmony search-based H-infinity control method for islanded microgrid. ISA Trans 2020;99:252–69.
[39] Hossain M, Pota H, Issa W, Hossain M. Overview of AC microgrid controls with inverter-interfaced generations. Energies 2017; 10(9).
[40] Roslan M, Hannan M, Ker P, Uddin M. Microgrid control methods toward achieving sustainable energy management. Appl Energy 2019;240:583–607.
[41] Sedhom Bishoy E, El-Saadawi Magdi M, Hatata Ahmed Y, Abd-Raboh El-Hosaini E. H-Infinity versus model predictive control methods for seamless transition between islanded and grid-connected modes of microgrid. IET Renew Power Gener 2020;14(5):856–70.
[42] Phan B, Lai Y. Control strategy of a hybrid renewable energy system based on reinforcement learning approach for an isolated microgrid. Appl Sci 2019; 9(19).
[43] Mahmoud M, Alyazidi N, Abouheaf M. Adaptive intelligent techniques for microgrid control systems: A survey. Int J Electr Power Energy Syst 2017;90:292–305.
[44] Xiao H, Pei W, Deng W, Kong L, Sun H, Tang C. A comparative study of deep neural network and meta-model techniques in behavior learning of microgrids. IEEE Access 2020;8:30104–18.
[45] Han Y, Ning X, Yang P, Xu L. Review of power sharing, voltage restoration and stabilization techniques in hierarchical controlled DC microgrids. IEEE Access 2019;7:149202–23.
[46] Zhou Q, Shahidehpour M, Paaso A, Bahramirad S, Alabdulwahab A, Abusorrah A. Distributed control and communication strategies in networked microgrids. IEEE Commun Surveys Tutorials 2020;22(4):2586–633.